

BAW-1638

May 1981

ANALYSIS OF CAPSULE V

Virginia Electric & Power Company
North Anna Unit No. 1

— Reactor Vessel Materials Surveillance Program —

Babcock & Wilcox

8408210393 840816
PDR ADOCK 05000338
P PDR

BAW-1638

May 1981

ANALYSIS OF CAPSULE V

Virginia Electric & Power Company
North Anna Unit No. 1

— Reactor Vessel Materials Surveillance Program —

by

A. L. Lowe, Jr., PE
W. A. Pavinich
J. K. Schmotzer
C. L. Whitmarsh

B&W Contract No. 582-7116

BABCOCK & WILCOX
Nuclear Power Group
Nuclear Power Generation Division
P. O. Box 1260
Lynchburg, Virginia 24505

Babcock & Wilcox

CONTENTS

| | Page |
|---|------|
| 1. INTRODUCTION | 1-1 |
| 2. POST-IRRADIATION TESTING | 2-1 |
| 2.1. Visual Examination and Inventory | 2-1 |
| 2.2. Thermal Monitors | 2-1 |
| 2.3. Tension Testing | 2-2 |
| 2.4. CVN Impact Testing | 2-2 |
| 3. DISCUSSION OF CAPSULE RESULTS | 3-1 |
| 3.1. Tensile Properties | 3-1 |
| 3.2. Charpy Impact Properties | 3-1 |
| 4. NEUTRON DOSIMETRY | 4-1 |
| 4.1. Introduction | 4-1 |
| 4.2. Analytical Approach | 4-2 |
| 4.3. Results | 4-3 |
| 4.4. Summary of Results | 4-5 |
| 5. SUMMARY OF RESULTS | 5-1 |
| 6. CERTIFICATION | 6-1 |
| 7. REFERENCES | 7-1 |
| APPENDIXES | |
| A. Surveillance Material Properties | A-1 |
| B. Preirradiation Tensile Data | B-1 |
| C. Preirradiation Charpy Impact Data | C-1 |
| D. Threshold Detector Information | D-1 |
| E. LRC-TP-78 | E-1 |
| F. LRC-TP-80 | F-1 |

List of Tables

| Table | Page |
|---|------|
| 2-1. Tensile Properties of North Anna Unit 1, Capsule V, Base and Weld Metals Irradiated to 2.49×10^{18} nvt | 2-3 |
| 2-2. Charpy Impact Data for North Anna Unit 1, Capsule V, Base Metal Irradiated to 2.49×10^{18} nvt | 2-3 |
| 2-3. Charpy Impact Data for North Anna Unit 1, Capsule V, Weld Metal Irradiated to 2.49×10^{18} nvt | 2-4 |
| 3-1. Comparison of Tensile Test Results | 3-4 |
| 3-2. Observed Vs Predicted Changes in Irradiated Charpy Impact Properties | 3-5 |
| 4-1. Surveillance Capsule Detectors | 4-5 |
| 4-2. Dosimeter Activations | 4-6 |
| 4-3. Neutron Flux and Fluence | 4-6 |
| 4-4. Predicted Lifetime Fluence to Pressure Vessel for $E > 1$ Mev | 4-7 |
| A-1. Heat Treatment History | A-2 |
| A-2. Quantitative Chemical Analysis, wt % | A-3 |
| B-1. Preirradiation Tensile Properties of Forging Material (Base Metal) and Weld Metal | B-2 |
| C-1. Preirradiation Charpy V-Notch Impact Data for North Anna Unit 1 Reactor Pressure Vessel Lower Shell Forging 03, Heat No. 990400/292332, Axial Orientation | C-2 |
| C-2. Preirradiation Charpy V-Notch Impact Data for North Anna Unit 1 Reactor Pressure Vessel Lower Shell Forging 03, Heat No. 990400/292332, Tangential Orientation | C-3 |
| C-3. Preirradiation Charpy V-Notch Impact Data for North Anna Unit 1 Reactor Pressure Vessel Core Region Weld Heat-Affected Zone Material | C-4 |
| C-4. Preirradiation Charpy V-Notch Impact Data for North Anna Unit 1 Reactor Pressure Vessel Core Region Weld Metal | C-5 |
| D-1. North Anna Neutron Dosimeters - Capsule V Irradiation Ended September 25, 1979, 24:00 | D-2 |
| D-2. Dosimeter Activation Cross Sections | D-4 |

List of Figures

| Figure | Page |
|--|------|
| 2-1. Charpy Impact Data From Irradiated Base Metal, Axial Orientation | 2-5 |
| 2-2. Charpy Impact Data From Irradiated Base Metal, Tangential Orientation | 2-6 |
| 2-3. Charpy Impact Data From Irradiated Weld Metal | 2-7 |
| 2-4. Charpy Impact Data From Irradiated Base Metal, Heat-Affected-Zone | 2-8 |
| 3-1. Irradiated Vs Unirradiated Charpy Impact Properties of Base Metal, Axial Orientation | 3-6 |
| 3-2. Irradiated Vs Unirradiated Charpy Impact Properties of Base Metal, Tangential Orientation | 3-7 |

Figures (Cont'd)

| Figure | Page |
|--|------|
| 3-3. Irradiated Vs Unirradiated Charpy Impact Properties of Weld Metal | 3-8 |
| 3-4. Irradiated Vs Unirradiated Charpy Impact Properties of Base Metal, Heat-Affected-Zone | 3-9 |
| 4-1. Relative Fast Flux at Specimen and Dosimeter Locations in Surveillance Capsule V | 4-7 |
| 4-2. Axial Shape of Fast Flux at the Pressure Vessel Surface | 4-8 |
| 4-3. Calculated Maximum End-of-Life Fluence as a Function of Penetration in the Pressure Vessel | 4-9 |
| 4-4. Azimuthal Variation of Fast Flux at the Pressure Vessel Surface | 4-10 |
| C-1. Charpy Impact Data From Unirradiated Base Metal, Axial Orientation | C-6 |
| C-2. Charpy Impact Data From Unirradiated Base Metal, Tangential Orientation | C-7 |
| C-3. Charpy Impact Data From Unirradiated Weld Metal | C-8 |
| C-4. Charpy Impact From Unirradiated Base Metal, Heat-Affected-Zone | C-9 |

1. INTRODUCTION

This report describes the results of the examination of the first capsule from the Virginia Electric Power Company's North Anna Unit No. 1 reactor vessel surveillance program. Capsule "V" is a part of the continuing surveillance program which monitors the effects of neutron irradiation on the reactor pressure vessel materials under actual operating conditions.

The specific objectives of the program are to monitor the effects of neutron irradiation on the tensile and impact properties of the reactor pressure vessel materials under actual operating conditions and to verify the fluence calculations to which the materials are exposed. The surveillance program for the North Anna Unit No. 1 reactor pressure vessel materials was designed and recommended by Westinghouse Electric Company. The surveillance program and the pre-irradiation mechanical properties of the reactor vessel materials are described in WCAP-8771.¹ The surveillance program was planned to cover the 40-year design life of the reactor pressure vessel and is based on ASTM E-185-73, Annex A1, "Standard Recommended Practice for Surveillance Tests for Nuclear Reactor Vessels."

This report summarizes the testing and the post-irradiation data obtained from the testing and analysis of the tensile and Charpy specimens as well as the evaluation of the thermal monitors. In addition, the dosimeters were measured and the fluence values for both the capsule materials and the reactor vessel were calculated. The wedge-opening-loading (WOL) specimens were not tested at this time and were placed in storage to be tested later if the need for the data develops.

2. POST-IRRADIATION TESTING

2.1. Visual Examination and Inventory

All samples were visually examined for signs of abnormalities. The contents of the capsule were inventoried and compared with the program characterization report inventory. All of the specimens were covered with a tightly adherent black substance of unknown origin. This condition may have been caused by residue from cleaning or from the capsule assembly. There was no evidence of rust or of the penetration of reactor coolant into the capsule.

The inventory of specimens was consistent with Figure 2-6 of the Westinghouse pre-irradiation report¹ with the exception of a discrepancy involving Charpy base metal specimens. This figure indicates 12 tangential (VT series) and 8 axial (VL series) specimens, while Table 2-1 of the same report shows 8 tangential and 12 axial specimens. The capsule actually contained 12 specimens marked "VT" and 8 marked "VL." For the post-irradiation data (Figures 2-2 and 2-3) to correlate with the pre-irradiation data (see Figures C-1 and C-2), it is necessary to assume that Table 2-1 was correct and that the VT specimens were axial in orientation and the VL specimens were transverse. Test data presented in this report (see Figures 3-1 and 3-2) support this assumption.

All flux wires and thermal monitors were also covered with the black substance mentioned earlier. As a result, Pyrex-encapsulated thermal monitors could not be visually examined.

2.2. Thermal Monitors

Surveillance capsule V contained a temperature monitor holder block containing two fusible alloys with different melting points. Because of the black substance, the Pyrex-encapsulated thermal monitors could not be visually examined. Consequently, they were radiographed for evaluation. Neither of the two thermal monitors were melted, although the low temperature monitor had slumped. From these data it was concluded that the irradiated specimens had

been exposed to a maximum temperature in the range of 579F or less during the reactor vessel operating period. There appeared to be no significant signs of a temperature gradient along the capsule length.

2.3. Tension Testing

All tension tests were conducted in accordance with Technical Procedure LRC-TP-78 (see Appendix E); four specimens were tested. One weld metal and one axial base metal specimen were tested at 550F. The other weld metal and axial base metal specimens were tested at room temperature. A constant displacement rate of 0.005 in./min was imposed on each specimen until fracture. Percent total elongation, percent reduction in cross-sectional area, 0.2% offset yield strength, and ultimate tensile strength were determined in accordance with ASTM E8-69 and A370-73. These data are presented in Table 2-1.

2.4. CVN Impact Testing

All impact tests were conducted in accordance with Technical Procedure LRC-TP-80 (see Appendix F). The four groups of specimens (axially oriented base metal, transversely oriented base metal, weld metal, and heat-affected zone metal) were tested at temperatures between -40 and 280F. Absorbed energy, test temperature, percent shear fracture, and lateral expansion were determined in accordance with ASTM Specifications E23-73 and A370-73. Plots of test temperature versus absorbed energy, percent shear, and lateral expansion were prepared for each specimen. These data are presented in Table 2-2 and Figures 2-1 through 2-4.

Table 2-1. Tensile Properties of North Anna Unit 1, Capsule V,
Base and Weld Metals Irradiated to 2.49×10^{18} nvt

| Specimen ID No. | Test temp., F | Strength, ksi | | Elongation, % | | Red'n of area, % |
|--------------------------------|---------------------|---------------|--------------|---------------|-------------|---------------------|
| | | Yield, YS | Ult., UTS | Uniform UE | Total TE | |
| <u>Base Metal - Transverse</u> | | | | | | |
| VT-3 | 76 | 80.4 | 99.3 | 12.0 | 20.9 | 54.9 |
| VT-4 | 548 | 64.7 | 95.7 | 10.0 | 18.4 | 47.0 |
| <u>Weld Metal</u> | | | | | | |
| VW-4 | 78 | 70.8 | 84.5 | 13.0 | 19.3 | 65.0 |
| VW-3 | 548 | 63.6 | 84.5 | 11.7 | 19.0 | 56.5 |

Table 2-2. Charpy Impact Data for North Anna Unit 1, Capsule V,
Base Metal Irradiated to 2.49×10^{18} nvt

| Specimen ID No. | Test temp., F | Abs. energy, ft-lb | Lat. exp., 10^{-3} in. | Shear fracture, % |
|--------------------------------|---------------------|-----------------------|-----------------------------|-------------------------|
| <u>Base Metal - Axial</u> | | | | |
| VT-19 | 0 | 12.5 | 7.0 | 0 |
| VT-14 | 40 | 15.5 | 11.5 | 0 |
| VT-16 | 60 | 29.0 | 23.5 | 14 |
| VT-13 | 73 | 39.0 | 29.0 | 0 |
| VT-22 | 100 | 40.0 | 32.0 | 34 |
| VT-15 | 120 | 41.0 | 35.0 | 42 |
| VT-24 | 130 | 51.0 | 42.0 | 38 |
| VT-18 | 140 | 59.0 | 48.0 | 98 |
| VT-23 | 160 | 60.0 | 50.0 | 98 |
| VT-21 | 195 | 79.0 | 66.0 | 100 |
| VT-20 | 240 | 68.5 | 60.0 | 100 |
| VT-17 | 280 | 77.0 | 68.0 | 100 |
| <u>Base Metal - Tangential</u> | | | | |
| VL-15 | 0 | 7.0 | 4.0 | 0 |
| VL-13 | 40 | 36.0 | 26.5 | 0 |
| VL-9 | 60 | 51.0 | 40.0 | 5 |
| VL-16 | 73 | 32.0 | 23.0 | 25 |
| VL-12 | 100 | 50.0 | 39.0 | 43 |

Table 2-2. (Cont'd)

| Specimen ID No. | Test temp., F | Abs. energy, ft-lb | Lat. exp., 10 ⁻³ in. | Shear fracture, % |
|--|---------------------|-----------------------|------------------------------------|-------------------------|
| VL-10 | 120 | 76.5 | 57.5 | 56 |
| VL-11 | 196 | 113.0 | 78.0 | 89 |
| VL-14 | 280 | 122.0 | 86.0 | 100 |
| <u>Base Metal - Heat-Affected Zone</u> | | | | |
| VH-18 | -40 | 66.0 | 48.0 | 3 |
| VH-13 | 0 | 19.5 | 8.0 | 10 |
| VH-16 | 40 | 22.5 | 15.0 | 60 |
| VH-19 | 50 | 16.5 | 15.0 | 40 |
| VH-20 | 60 | 49.5 | 30.5 | 89 |
| VH-23 | 73 | 89.0 | 66.0 | 62 |
| VH-21 | 100 | 81.0 | 55.0 | 71 |
| VH-15 | 120 | 67.5 | 42.0 | 55 |
| VH-24 | 160 | 93.0 | 67.0 | 99 |
| VH-22 | 198 | 105.0 | 71.0 | 100 |
| VH-14 | 240 | 113.0 | 70.0 | 100 |
| VH-17 | 280 | 102.0 | 74.0 | 100 |

Table 2-3. Charpy Impact Data for North Anna Unit 1, Capsule V, Weld Metal Irradiated to 2.49×10^{18} nvt

| Specimen ID No. | Test temp., F | Abs. energy, ft-lb | Lat. exp., 10 ⁻³ in. | Shear fracture, % |
|--------------------|---------------------|-----------------------|------------------------------------|-------------------------|
| VW-20 | -40 | 4.5 | 4.5 | 0 |
| VW-22 | 0 | 25.0 | 25.5 | 50 |
| VW-24 | 40 | 26.0 | 29.0 | 46 |
| VW-17 | 60 | 33.0 | 31.5 | 28 |
| VW-16 | 73 | 39.0 | 31.0 | 34 |
| VW-23 | 90 | 47.0 | 49.0 | 89 |
| VW-21 | 100 | 60.0 | 56.0 | 25 |
| VW-14 | 120 | 73.0 | 62.0 | 72 |
| VW-15 | 160 | 62.5 | 52.5 | 96 |
| VW-18 | 198 | 92.5 | 73.0 | 100 |
| VW-13 | 240 | 100.0 | 80.0 | 100 |
| VW-19 | 280 | 87.0 | 77.0 | 100 |

Figure 2-1. Charpy Impact Data From Irradiated Base Metal, Axial Orientation

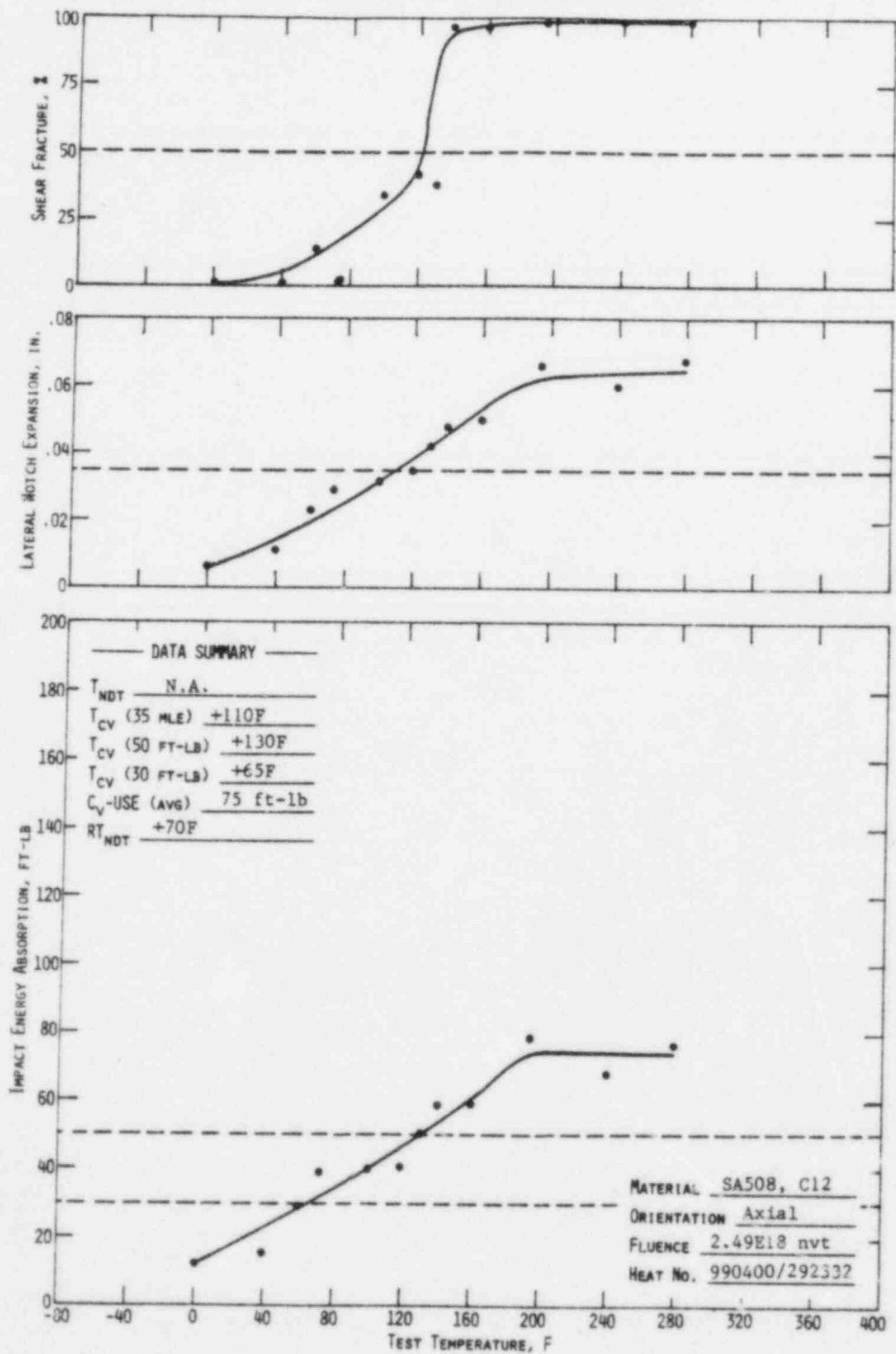


Figure 2-2. Charpy Impact Data From Irradiated Base Metal, Tangential Orientation

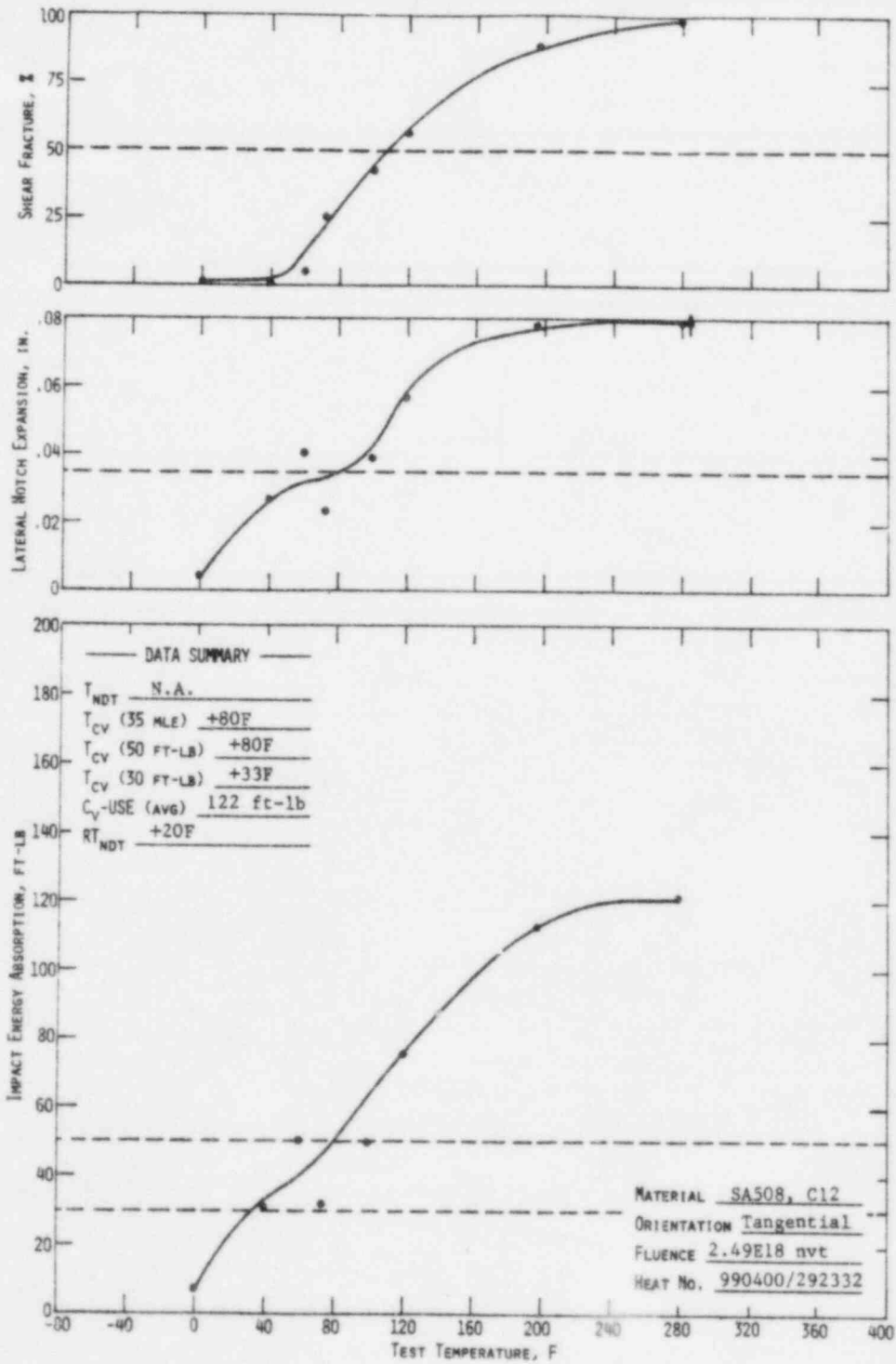


Figure 2-3. Charpy Impact Data From Irradiated Weld Metal

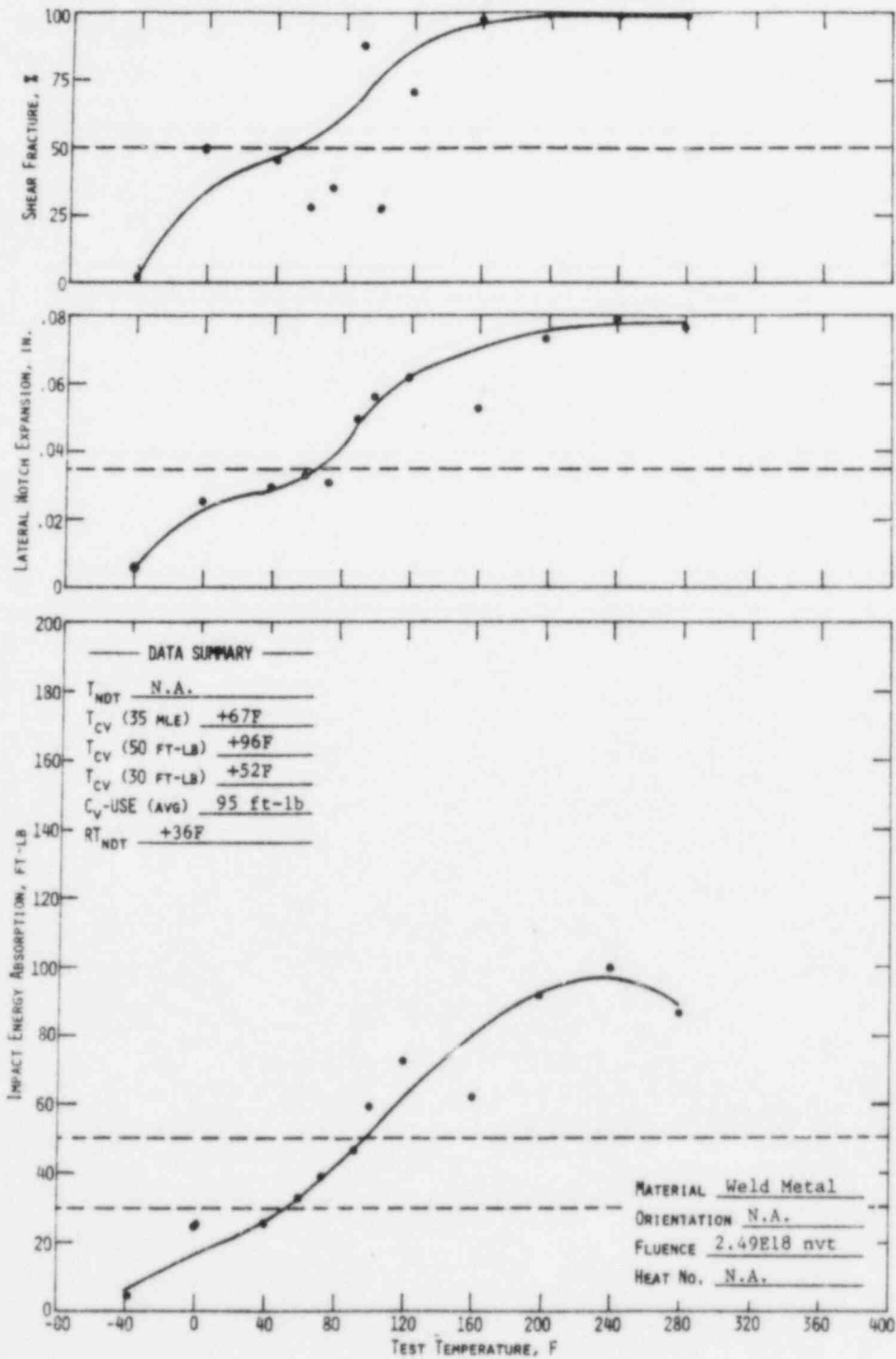
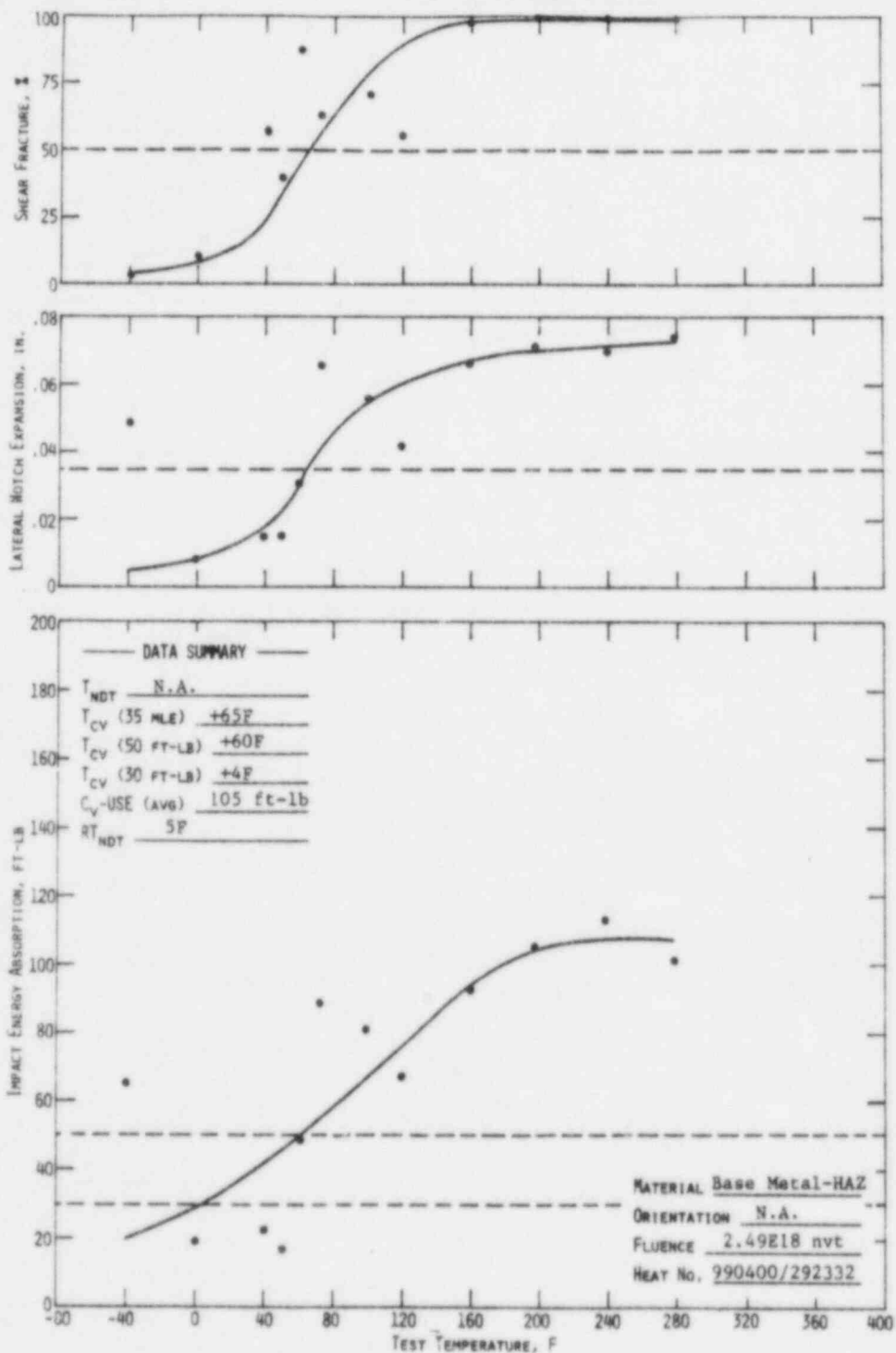


Figure 2-4. Charpy Impact Data From Irradiated Base Metal, Heat-Affected-Zone



3. DISCUSSION OF CAPSULE RESULTS

3.1. Tensile Properties

Table 3-1 compares irradiated and unirradiated tensile properties. At both ambient and elevated temperatures, the ultimate and yield strength changes in the base metal as a result of irradiation and the corresponding changes in ductility are within the range expected. There is some strengthening, as indicated by increases in ultimate and yield strength and small decreases in ductility properties. Some of the changes observed in the weld metal are so small as to be considered within experimental error. The changes in the properties of the base metal at both room temperature and 550F are greater than those observed for the weld metal, indicating a greater sensitivity of the base metal to irradiation damage. These observations are further supported by the fact that the base metal chemistry contains more of those elements that influence radiation sensitivity than are contained in the weld metal. It should be noted that the relative irradiation sensitivity of the two materials was found to be reversed from that normally observed in these data. However, the number of tensile specimens is appropriately limited, which could affect the statistical significance of the data and thus not reflect the long-term behavior of the materials.

In either case, the changes in tensile properties are not significant relative to the analysis of the reactor vessel materials at this period in service life since the Charpy data govern the adjustment to pressure-temperature heatup and cooldown curves.

3.2. Charpy Impact Properties

The behavior of the Charpy V-notch impact data is more significant to the calculation of the reactor system's operating limitations. Table 3-2 compares the observed changes in irradiated Charpy impact properties with the predicted changes as shown in Figures 3-1 through 3-4.

The 50-ft-lb transition temperature shift for the base metal was slightly less than the shift that would be predicted according to Regulatory Guide 1.99. This means that the Regulatory Guide is a conservative predictor for the base metal. However, the weld metal shift was greater than the shift that would be predicted using Regulatory Guide 1.99. Similar differences were observed for the 30-ft-lb transition temperature shift except that the magnitude of difference between the observed and predicted increased relative to the differences at the 50-ft-lb level.

The less-than-ideal comparison may be attributed to the spread in the data of the unirradiated material combined with the fact that there was a minimum of data points to establish the irradiated curve. These two variables can contribute to increasing the error between the observed and predicted values. Under these conditions, the comparison indicates that the estimating curves in RC 1.99 for medium-copper materials at medium fluence levels are conservative for predicting the 50-ft-lb transition temperature shifts. The estimating curves for high-copper material at medium fluence levels are not in good agreement with the observed data and do not conservatively predict the expected shift values.

The increase in the 35-mil lateral expansion transition temperature is compared with the shift in RT_{NDT} curve data in a manner similar to the comparison made for the 50-ft-lb transition temperature shift. These data show behavior similar to that seen in the comparison of the observed and predicted 50-ft-lb transition data.

The data for the decrease in Charpy USE with irradiation showed good agreement with predicted values for the base metal. However, the weld metal data compare well with the predicted value. In view of the lack of data for low-copper weldments at the low to medium fluence values that were used to develop the estimating curves, the predictive techniques should improve as additional data are obtained from which better prediction curves can be developed.

Results from other capsules indicate that the RT_{NDT} estimating curves have greater inaccuracies at the low neutron fluence levels ($\leq 5 \times 10^{18}$ n/cm²). This inaccuracy is attributed to the limited data at the low fluence values and to the fact that the majority of the data used to define the curves in RG 1.99 are based on the shift at 30-ft-lb as compared to the current requirement of 50-ft-lb. For most materials, the shifts measured at 50-ft-lb/35 MLE are

expected to be higher than those measured at 30-ft-lb. The significance of the shifts at 50-ft-lb and/or 35 MLE is not well understood at present, especially for materials having USEs that approach the 50-ft-lb level and/or the 35-MLE level. Materials with this characteristic may have to be evaluated at transition energy levels lower than 50 ft-lb.

The lack of good agreement of the change in Charpy USE is further support of the inaccuracy of the prediction curves at the lower fluence levels. Although the prediction curves are conservative in that they predict a larger drop in USE certain materials than are observed for a given fluence and copper content, the conservatism can unduly restrict the operational limitations. These data support the contention that the USE drop curves will have to be modified as more reliable data become available; until that time the design curves used to predict the decrease in USE have adequate conservatism.

Table 3-1. Comparison of Tensile Test Results

| | <u>Room temp test</u> | | <u>Elevated temp test</u> | |
|---|-----------------------|--------------|---------------------------|-------------|
| | <u>Unirr</u> | <u>Irrad</u> | <u>550F</u> | <u>548F</u> |
| <u>Base Metal</u> ^(a) | | | | |
| Fluence, 10^{18} n/cm ² (>1 MeV) | 0 | 2.49 | 0 | 2.49 |
| Ult. tensile strength, ksi | 92.5 | 99.3 | 86.2 | 95.7 |
| 0.2% yield strength, ksi | 70.7 | 80.4 | 55.6 | 64.7 |
| Elongation, % | 18.8 | 20.9 | 23.3 | 18.4 |
| RA, % | 58.8 | 54.9 | 54.5 | 47.0 |
| <u>Weld Metal</u> | | | | |
| Fluence, 10^{18} n/cm ² (>1 MeV) | 0 | 2.49 | 0 | 2.49 |
| Ult. tensile strength, ksi | 79.4 | 84.5 | 78.7 | 84.5 |
| 0.2% yield strength, ksi | 64.2 | 70.8 | 60.9 | 63.6 |
| Elongation, % | 19.2 | 19.3 | 19.0 | 19.0 |
| RA, % | 71.0 | 65.0 | 60.0 | 56.5 |

(a) Transverse-axial.

Table 3-2. Observed Vs Predicted Changes in Irradiated Charpy Impact Properties

| <u>Material</u> | <u>Observed</u> | <u>Predicted</u> ^(a) |
|---|-----------------|---------------------------------|
| <u>Increase in 30-ft-lb trans temp, F</u> | | |
| Base material | | |
| Axial | 21 | 87 |
| Tangential | 39 | 87 |
| Heat-affected zone | 55 | 87 |
| Weld metal | 78 | 53 |
| <u>Increase in 50-ft-lb trans temp, F</u> | | |
| Base material | | |
| Axial | 45 | 87 |
| Tangential | 68 | 87 |
| Heat-affected zone | 58 | 87 |
| Weld metal | 71 | 53 |
| <u>Increase in 35-MLE trans temp, F</u> | | |
| Base material | | |
| Axial | 36 | 87 ^(b) |
| Tangential | 73 | 87 ^(b) |
| Heat-affected zone | 45 | 87 ^(b) |
| Weld metal | 80 | 53 ^(b) |
| <u>Decrease in Charpy USE, ft-lb</u> | | |
| Base material | | |
| Axial | 10 | 14 |
| Tangential | 25 | 22 |
| Heat-affected zone | 40 | 19 |
| Weld metal | 3 | 15 |

(a) These values predicted per Regulatory Guide 1.99, Revision 1.

(b) Based on the assumption that MLE as well as 50-ft-lb transition temperature is used to control the shift in RT_{NDT} .

Figure 3-1. Irradiated Vs Unirradiated Charpy Impact Properties of Base Metal, Axial Orientation

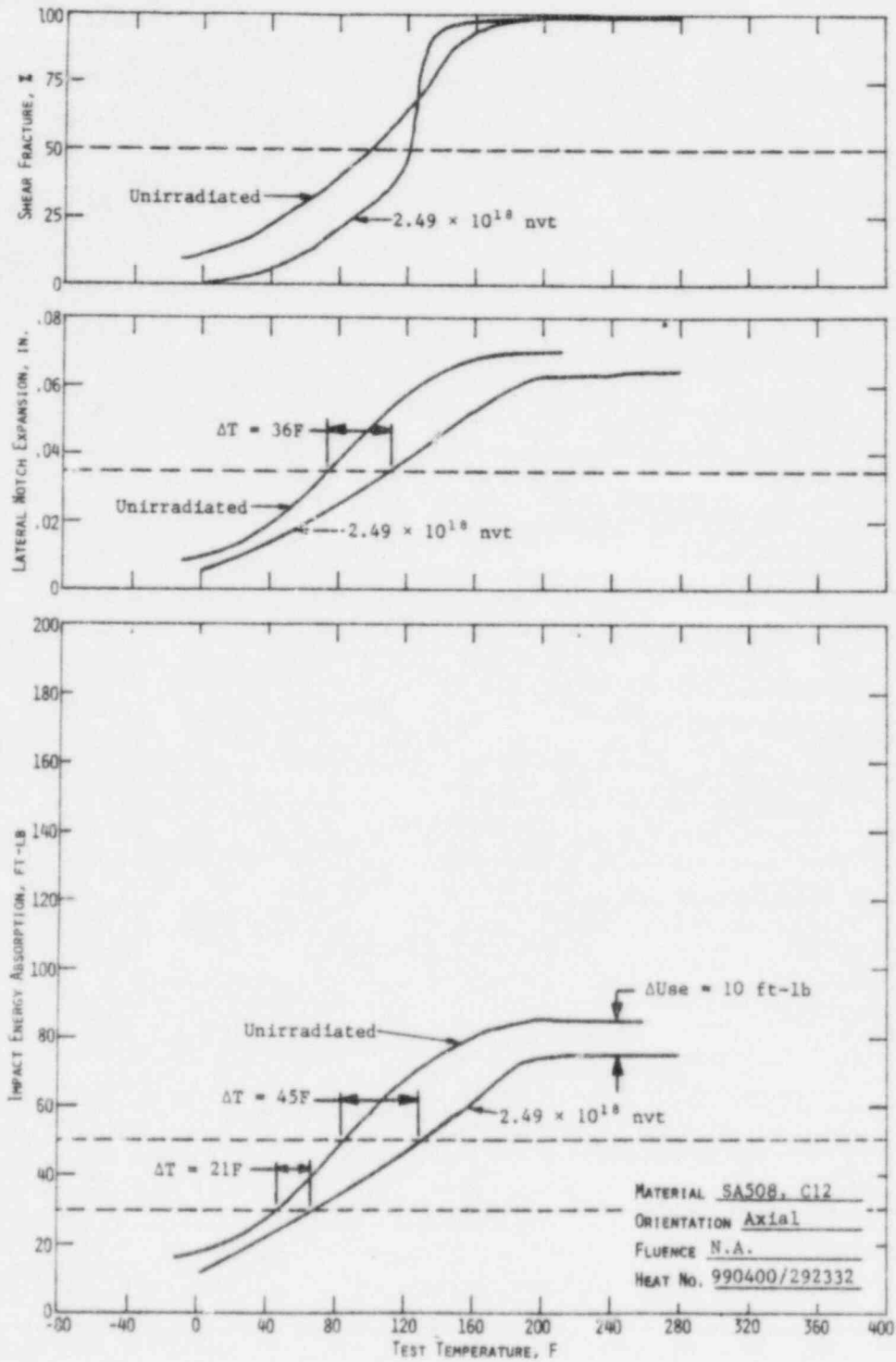


Figure 3-2. Irradiated Vs Unirradiated Charpy Impact Properties of Base Metal, Tangential Orientation

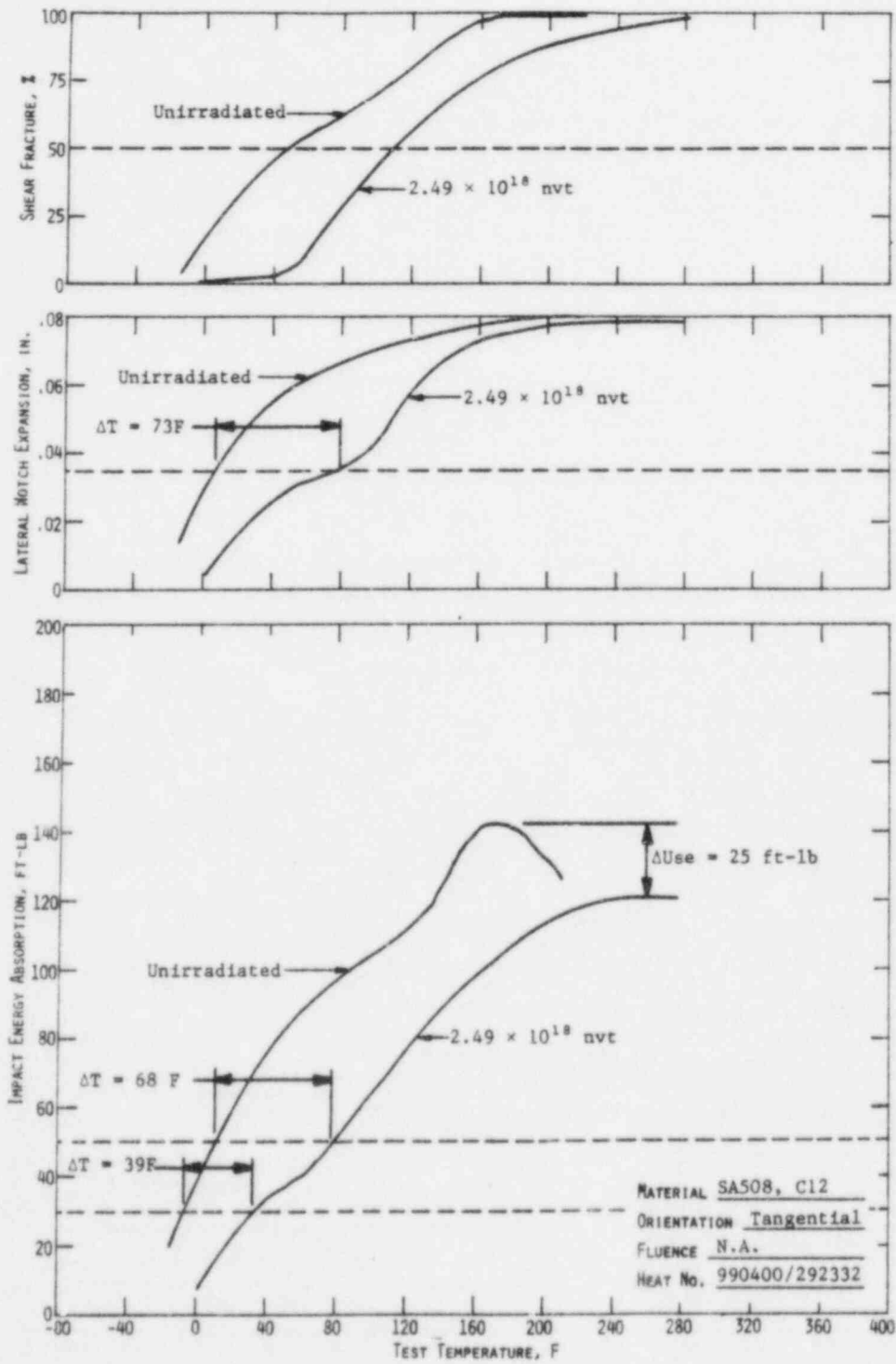


Figure 3-3. Irradiated Vs Unirradiated Charpy Impact Properties of Weld Metal

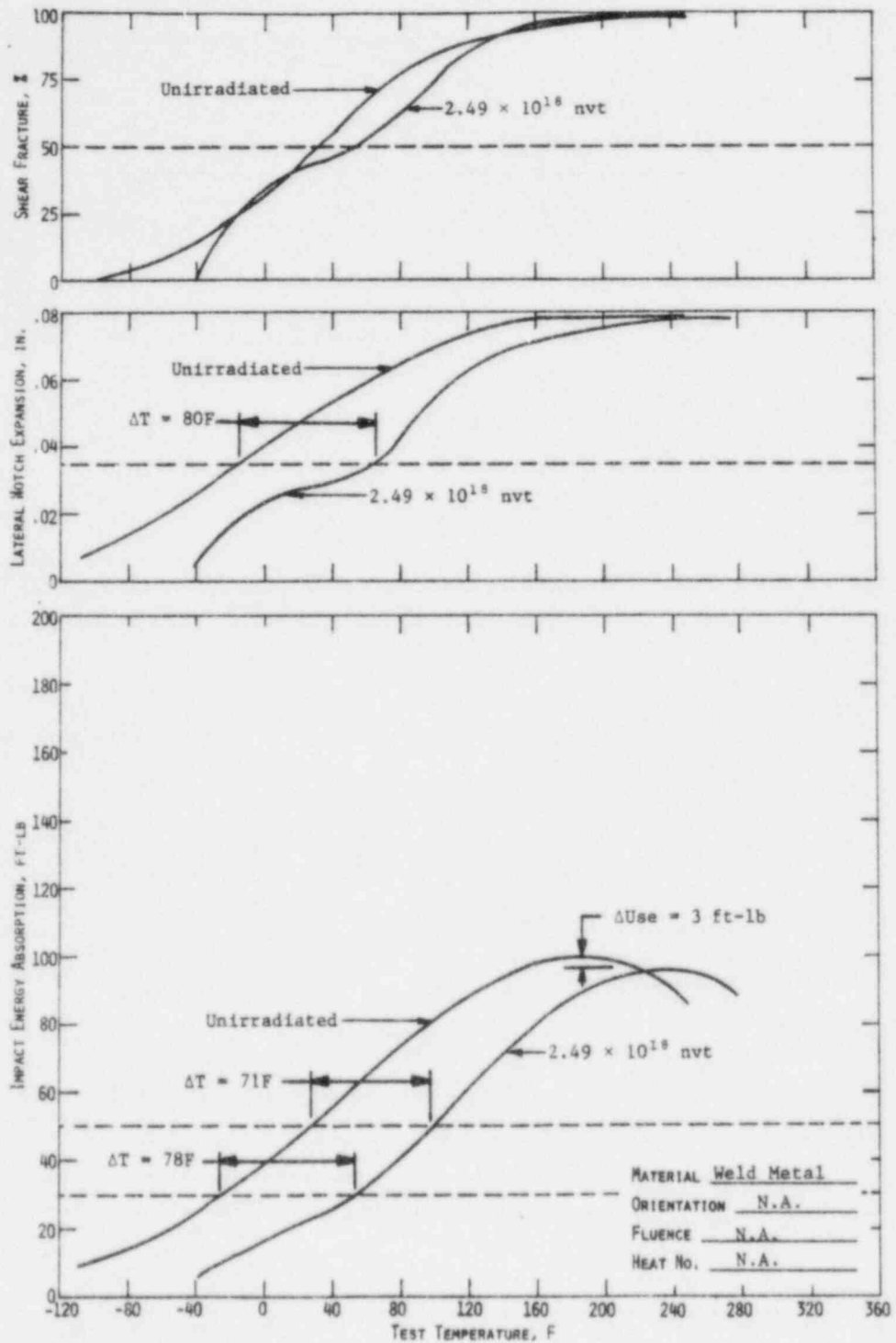
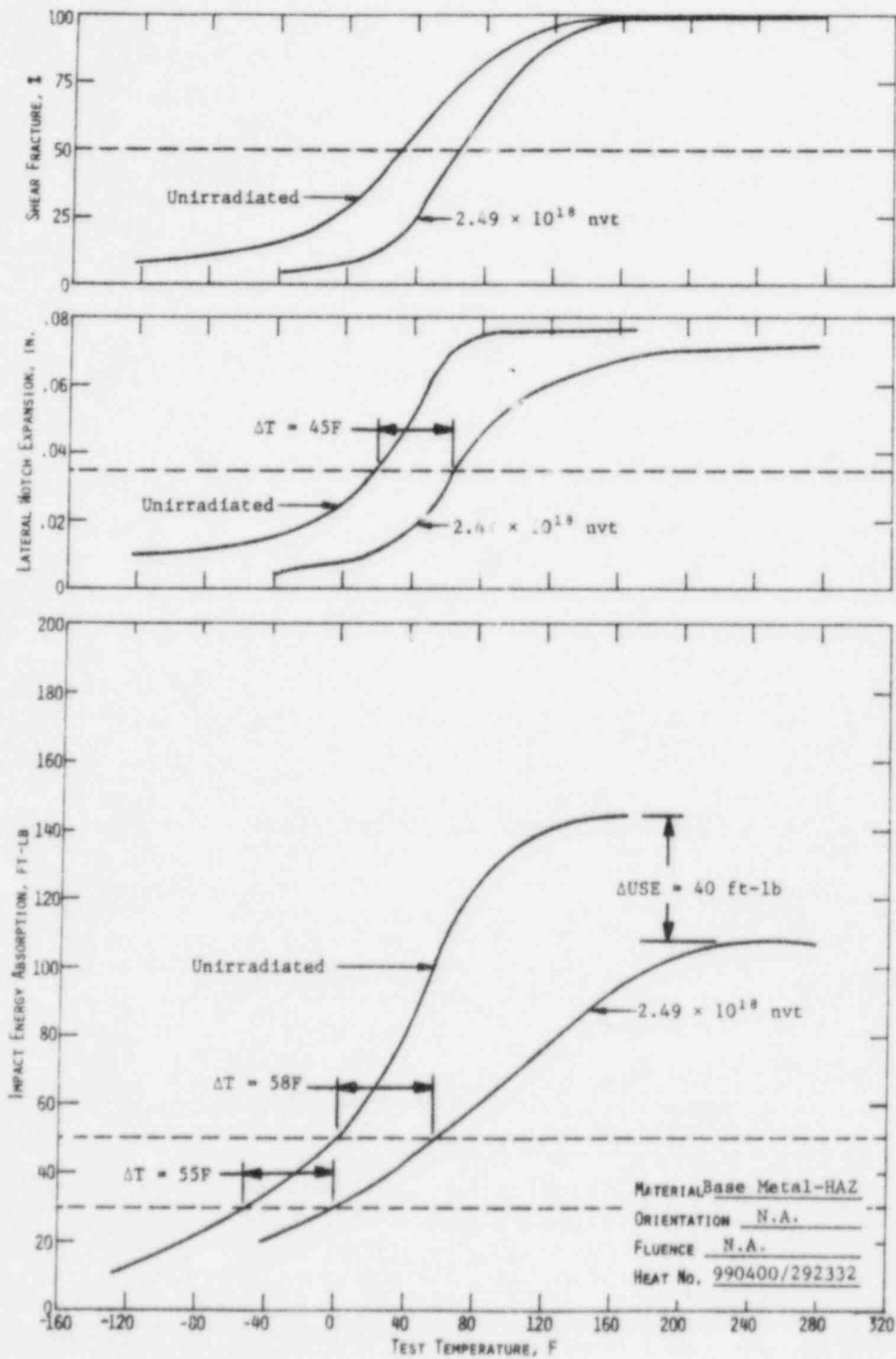


Figure 3-4. Irradiated Vs Unirradiated Charpy Impact Properties of Base Metal, Heat-Affected-Zone



4. NEUTRON DOSIMETRY

4.1. Introduction

A significant aspect of the surveillance program is to provide a correlation between the neutron fluence above 1 Mev and the radiation-induced property changes noted in surveillance specimens. To permit such a correlation, activation detectors with reaction thresholds in the energy range of interest are placed in each surveillance capsule. The reactions of interest for the detectors are given in Table 4-1.

Because of a long half-life of 30 years and an effective energy range of >0.5 Mev, the measurements of ^{137}Cs production from fission reactions in ^{237}Np and ^{238}U are more directly applicable than the other dosimeter reactions to analytical determinations of fast ($E > 1$ MeV) fluence during cycle 1. The other dosimeter reactions are useful as corroborating data for shorter time intervals and/or higher energy fluxes. Short-lived isotope activities are representative of reactor conditions over the latter portion of the irradiation period (full cycle) only, whereas reactions with a threshold energy > 3 or 4 Mev do not record a significant part of the total fast flux.

The energy-dependent neutron flux is not directly available from activation detectors because the dosimeters record only the integrated effect of the neutron flux on the target material as a function of both irradiation time and neutron energy. To obtain an accurate estimate of the time-average of neutron flux incident upon the detector, the following parameters must be known: the operating history of the reactor, the energy response of the given detector, and the neutron spectrum at the detector location. Of these parameters, the definition of the neutron spectrum is the most difficult to obtain. Essentially, two means are available to obtain the spectrum: iterative unfolding of experimental foil data and analytical methods. Due to a lack of sufficient threshold detectors satisfying both the threshold energy and half-life requirements necessary for a surveillance program, calculated spectra are used in this analysis.

4.2. Analytical Approach

Energy-dependent neutron fluxes at the detector locations were determined by a discrete ordinates solution of the Boltzmann transport equation with the two-dimensional code DOT 35.² The North Anna 1 reactor was modeled from the core out to the primary concrete shield in R-theta geometry (based on a plan view along the core midplane and one-eighth core symmetry in the azimuthal dimension). Also included was an explicit model of a surveillance capsule at the proper location. The center of capsule V was positioned 192.84 cm from the core center and 15.0° off-axis. The reactor model contained the following regions: core, liner, bypass coolant, core barrel, inlet coolant, thermal shield, pressure vessel, cavity, and shield tank. Input parameters to the code included a pin-by-pin, time-averaged power distribution, CASK23E 22-group microscopic neutron cross sections³, S₈ order of angular quadrature, and P₃ expansion of the scattering cross section matrix.

Because of computer storage limitations, it was necessary to use 2 geometric models to cover the distance from the core to the primary shield. A boundary source output from the initial model A (core into the pressure vessel) was used to "bootstrap" a model B, which included the capsule.

Flux output from the DOT 35 calculations required only an axial distribution adjustment. Thus, fluxes were multiplied by an axial shape factor to account for the capsule elevation. Capsule V extended about 50 inches above and below the core midplane. This factor ranged from 1.06 to 1.19 for various dosimeter locations in the capsule and was 1.20 at the maximum location in the pressure vessel.

The calculation described above provides the neutron flux as a function of energy at the detector position. These calculated data are used in the following equations to obtain the calculated activities used for comparison with the experimental values. The basic equation for the activity D (in μCi/g) is given below.

$$D_i = \frac{CN}{A_i 3.7 \times 10^4} f_i \sum_E \sigma_n(E) \phi(E) \sum_{j=1}^M F_j \left(1 - e^{-\lambda_i \tau_j} \right) e^{-\lambda_i (T - \tau_j)} \quad (4-1)$$

where

C = normalizing constant, ratio of measured to calculated flux,

N = Avogadro's number,

A_i = atomic weight of target material i,

f_i = either weight fraction of target isotope in nth material or fission yield of desired isotope,

$\sigma_n(E)$ = group-averaged cross sections for material n, listed in Table D-3,

$\phi(E)$ = group-averaged fluxes calculated by DOT analysis,

F_j = fraction of full power during jth time interval, t_j ,

λ_i = decay constant of ith material,

t_j = interval of power history,

T = sum of total irradiation time, i.e., residual time in reactor, and wait time between reactor shutdown and counting,

τ_j = cumulative time from reactor startup to end of jth time period, i.e.,

$$\tau_j = \sum_{k=1}^j t_k.$$

The normalizing constant C can be obtained by equating the right side of equation 4-1 to the measured activity. With C specified, the neutron fluence greater than 1 Mev can be calculated from

$$\phi(E > 1.0 \text{ Mev}) = C \sum_{E=1}^{15 \text{ Mev}} \phi \sum_{j=1}^M F_j t_j \quad (4-2)$$

where M is the number of irradiation time intervals; the other values are as defined above.

4.3. Results

Calculated activities are compared to dosimeter measurements in Table 4-2. The fission wire data indicate about a 20% underprediction of fast flux ($E > 1 \text{ Mev}$) by the analytical mode described herein; non-fission wires were within -4 to +12% of measurements. Although many factors could account for this discrepancy, including the presence of impurities in the wires and possible

gamma-induced fission reactions, the comparison was considered good for this type of problem. Fission wire data were corroborated with additional fission product reactions not reported here. A value of 1.15 was conservatively selected for the normalization factor and then applied to calculated fluxes in the pressure vessel. Thus, fast flux ($E > 1$ Mev) was determined to be 6.98 (+10) n/cm^2-s in the capsule (center dosimeter location at core midplane) and 6.76 (+10) n/cm^2-s in the pressure vessel at the maximum location (Table 4-3). Corresponding fluence values for cycle 1 (413 EFPD at 2775 MW) were 2.49 (+18) and 2.41 (+18) n/cm^2 , respectively. Flux exposures for $E > 0.1$ Mev were greater by more than a factor of two. The maximum location in the pressure vessel was at the inside surface along a major axis (across the flats diameter) and about 80 cm below core midplane. The capsule lead factor (ratio of fast flux in the capsule to maximum fast flux in the pressure vessel) was 1.03 based on a central capsule location.

Flux magnitude is sensitive to location within an object as large as a surveillance capsule. Therefore, sufficient detail was included in the calculational model to provide flux values that were spatially averaged over each specimen. Data presented in Figure 4-1 show a difference of more than 25% between maximum and minimum specimen fluence (or flux) at the same elevation. The effect of axial position can be seen in Figure 4-2. Thus, the midplane values listed in Table 4-3 can be converted to other locations within a capsule by a radial factor (Figure 4-1) and a ratio of axial factors, local to midplane (Figure 4-2).

Cycle 1 fluence was extrapolated to the 32-year vessel design life by assuming proportionality to fast flux escaping the core from fuel management criticality analyses of cycles 2 through 4. Cycle 4 was presumed to be representative of an equilibrium cycle. This procedure accounts for the changes in relative power distribution resulting from fuel shuffling between fuel cycles and effectively translates cycle 1 results to equilibrium cycle results. Lifetime fluences at several pressure vessel locations are listed in Table 4-4. Fluence as a function of penetration through the pressure vessel is shown in Figure 4-3.

To facilitate estimation of flux (and/or fluence) at other capsule locations, the azimuthal variation of fast flux is plotted in Figure 4-4. Although the data were calculated at the vessel surface, they should also be applicable at

the capsule radius. Since all other capsule locations are located at angles over 15° off axis, the corresponding lead factors will be less than the capsule V lead factor.

4.4. Summary of Results

1. The average fast fluence at the capsule center for the midplane elevation was 2.49×10^{18} n/cm ($E > 1$ Mev) after the first fuel cycle (413 EFPD). The maximum value at the pressure vessel wall was calculated to be 2.41×10^{18} n/cm².
2. Extrapolation to the 32-year vessel design life based on assumed equilibrium cycle conditions resulted in values of 5.8 (+19), 3.4 (+18), and 8.5 (+18) n/cm² for maximum locations at the vessel surface, at T/4, and at 3T/4, respectively.

Table 4-1. Surveillance Capsule Detectors

| <u>Detector reaction</u> | <u>Energy range, Mev</u> | <u>Isotope half-life</u> |
|--|--------------------------|--------------------------|
| $^{54}\text{Fe}(n,p)^{54}\text{Mn}$ | >2.5 | 313 days |
| $^{58}\text{Ni}(n,p)^{58}\text{Co}$ | >2.3 | 71.2 days |
| $^{63}\text{Cu}(n,\alpha)^{60}\text{Co}$ | >5.0 | 5.27 years |
| $^{238}\text{U}(n,f)^{137}\text{Cs}$ | >1.1 | 30.1 years |
| $^{237}\text{Np}(n,f)^{137}\text{Cs}$ | >0.5 | 30.1 years |

Table 4-2. Dosimeter Activations

| <u>Reaction</u> | <u>A</u> measured activity, $\mu\text{Ci/g}$ | <u>B</u> calculated activity, $\mu\text{Ci/g}$ | <u>C = A/B</u> normalization constant |
|--|---|---|---|
| $^{54}\text{Fe}(n,p)^{54}\text{Mn}$ | 891 (a) | 964 | 0.92 |
| $^{58}\text{Ni}(n,p)^{58}\text{Co}$ | 1550 (b) | 1630 | 0.95 |
| $^{63}\text{Cu}(n,\alpha)^{60}\text{Co}$ | 2.08 | 2.58 | 0.81 |
| $^{238}\text{U}(n,f)^{137}\text{Cs}$ | 3.28 | 2.85 | 1.15 |
| $^{237}\text{Np}(n,f)^{137}\text{Cs}$ | 21.3 | 18.7 | 1.14 |

(a) Average of five dosimeter wires from Table D-2.

(b) Average of three dosimeter locations in calculational model.

Table 4-3. Neutron Flux and Fluence

| | <u>Fast flux,</u> $\text{n/cm}^2\text{-s}$ | <u>Fast fluence for</u> cycle 1 (413 EFPD), n/cm^2 |
|--|---|---|
| <u>E > 1 Mev</u> | | |
| Capsule, central dosimeter loc 'n (a) | 6.98 (+10) | 2.49 (+18) |
| Pressure vessel surface (max) | 6.76 (+10) | 2.41 (+18) |
| <u>E > 0.1 Mev</u> | | |
| Capsule, central dosimeter loc 'n | 1.72 (+11) | 6.14 (+18) |
| Pressure vessel surface (max) | 1.72 (+11) | 6.14 (+18) |

(a) Approximate geometric center of specimens at core midplane.

Table 4-4. Predicted Lifetime Fluence to Pressure Vessel for $E > 1$ Mev

| | Vessel surface | T/4 | 3T/4 |
|------------------------------|----------------|-----------|-----------|
| Average fast flux, n/cm^2s | 5.7 (+10) | 3.4 (+10) | 8.4 (+9) |
| Fast fluence, n/cm^2 | 5.8 (+19) | 3.4 (+19) | 8.5 (+18) |

Figure 4-1. Relative Fast Flux at Specimen and Dosimeter Locations in Surveillance Capsule V

| | | | |
|--------------------|--------|-----------|-----------|
| | Spacer | Specimen | Specimen |
| | | 1.05 | 0.86 |
| Core + | | A 1.09 | B 1.00 |
| | | Specimen | Specimen |
| ↓ Major Axis | | 1.10 | 0.91 |

A,B,C: Dosimeter wire positions.

Figure 4-2. Axial Shape of Fast Flux at the Pressure Vessel Surface

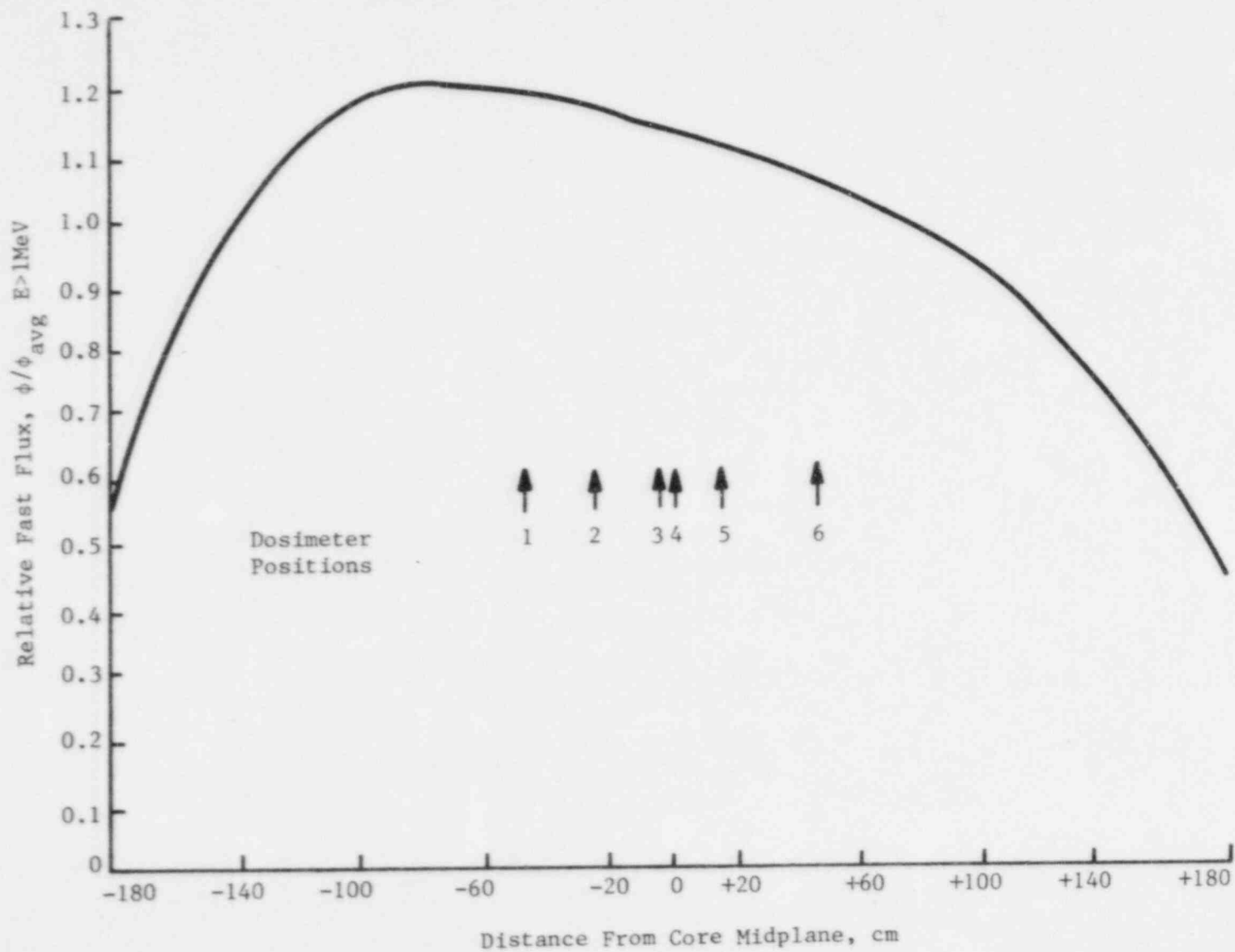


Figure 4-3. Calculated Maximum End-of-Life Fluence as a Function of Penetration in the Pressure Vessel

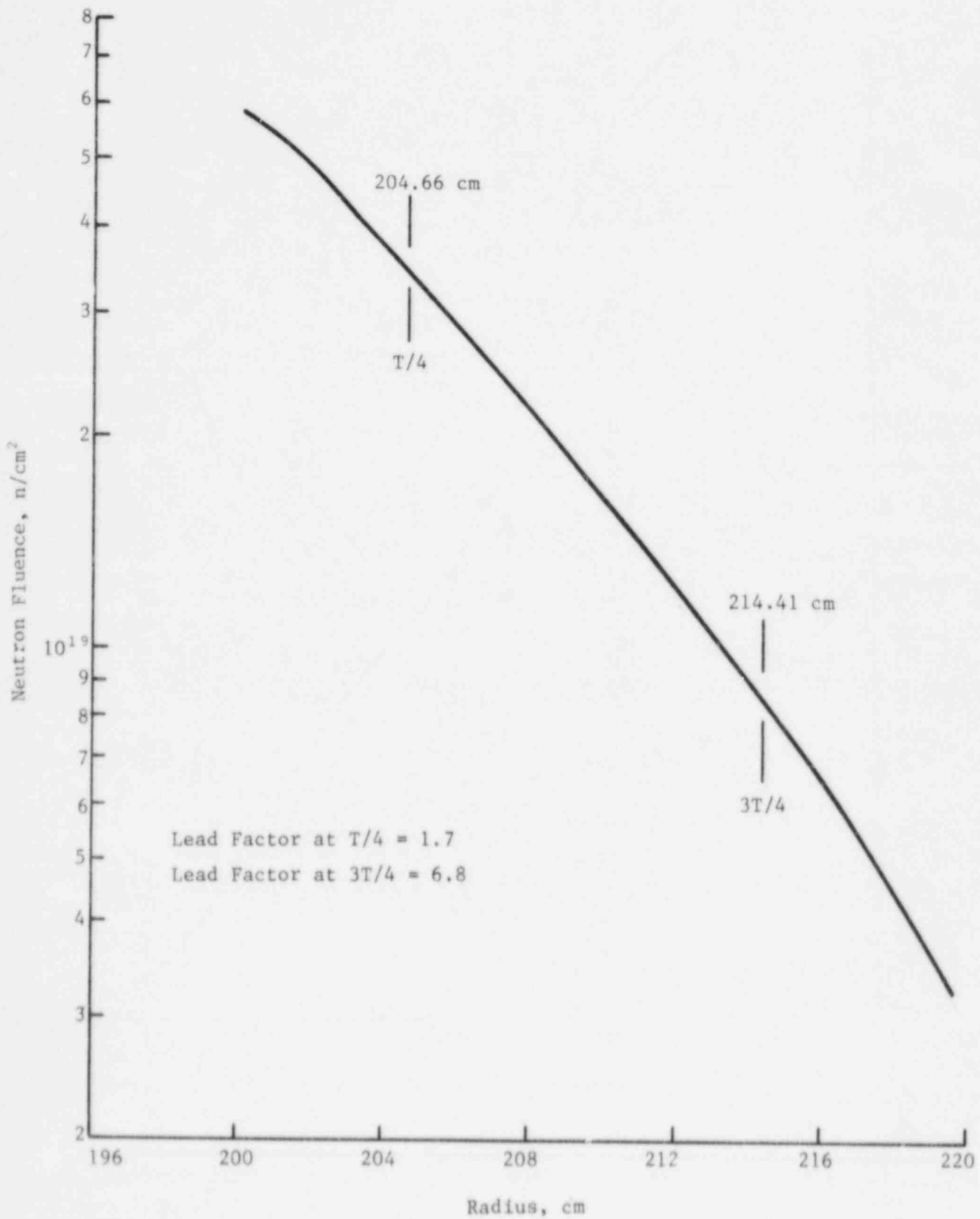
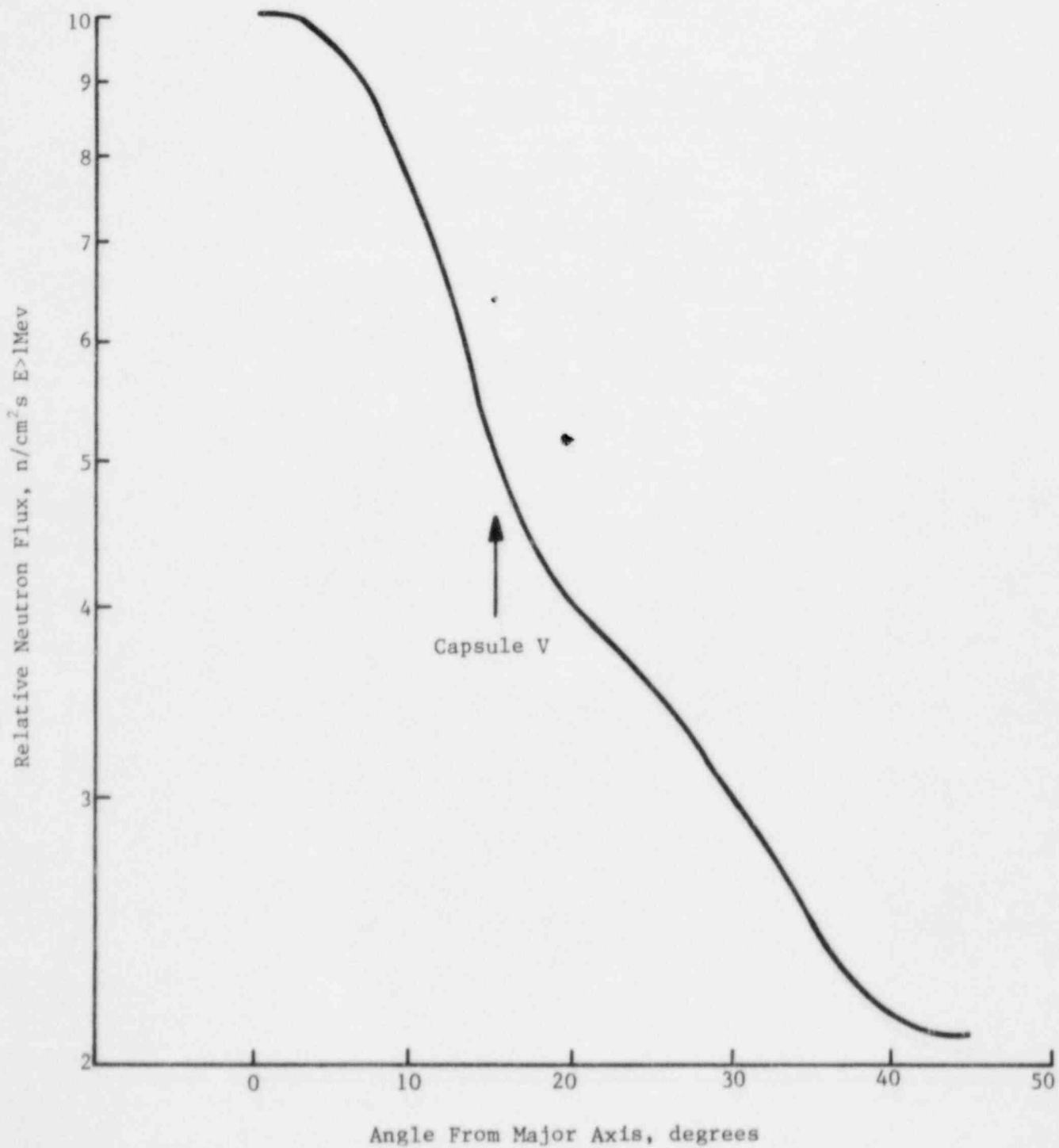


Figure 4-4. Azimuthal Variation of Fast Flux at the Pressure Vessel Surface



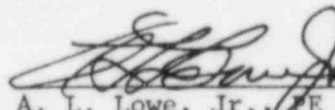
5. SUMMARY OF RESULTS

The analysis of the reactor vessel material contained in North Anna Unit 1, Capsule V, led to the following conclusions:


1. The capsule received an average fast fluence of 2.49×10^{18} n/cm² (E > 1 Mev). The predicted fast fluence for the reactor vessel T/4 location at the end of the first fuel cycle is 1.41×10^{18} n/cm² (E > 1 Mev).
2. The fast fluence of 2.49×10^{18} n/cm² (E > 1 Mev) increased the RT_{NDT} of the reactor vessel core region shell materials in the capsule to a maximum of 70F.
3. Based on the ratio of the fast flux at the surveillance capsule location to that at the vessel wall and an 80% load factor, the projected fast fluence the North Anna Unit 1 reactor pressure vessel will receive in 32 EPFY operation is 5.8×10^{19} n/cm² (E > 1 Mev).
4. The increase in the RT_{NDT} for the base plate material was conservative compared to that predicted by the currently used design curves of Δ RT_{NDT} versus fluence.
5. The increase in the RT_{NDT} for the weld metal was not in good agreement with that predicted by the currently used design curves of Δ RT_{NDT} versus fluence.
6. The current techniques used for predicting the change in Charpy impact upper shelf properties due to irradiation are conservative considering the difficulties in accurately defining the upper shelf.
7. The analysis of the neutron dosimeters demonstrated that the analytical techniques used to predict the neutron flux and fluence were accurate.
8. The thermal monitors indicated that the capsule design was satisfactory for maintaining the specimens within the desired temperature range.

6. CERTIFICATION

The specimens were tested, and the data obtained from Virginia Electric & Power Company's North Anna Unit 1 surveillance capsule V were evaluated using accepted techniques and established standard methods and procedures in accordance with the requirements of 10 CFR 50, Appendixes G and H.

 P.E. 20 March 1981
A. L. Lowe, Jr., P.E. Date
Project Technical Manager

This report has been reviewed for technical content and accuracy.

 5/11/81
J. D. Aadland Date
Component Engineering

7. REFERENCES

- ¹ J. A. Davidson and J. H. Phillips, Virginia Electric & Power Company North Anna Unit 1 Reactor Vessel Radiation Program, WCAP-8771, Westinghouse, Pittsburgh, September 1976.
- ² DOT 3.5 - Two-Dimensional Discrete Ordinates Radiation Transport Code, (CCC-276), Oak Ridge National Laboratory, WANL-TME-1982, December 1969.
- ³ CASK - 40-Group Coupled Neutron and Gamma-Ray Cross Section Data, Radiation Shielding Information Center, RSIC-DLC-23.

APPENDIX A
Surveillance Material Properties¹

The Rotterdam Dockyard Company supplied the Westinghouse Electric Corporation with sections of SA508 Class 2 forging used in the core region of the North Anna Unit No. 1 reactor pressure vessel for the Reactor Vessel Radiation Surveillance Program. The sections of material were removed from a 10-inch lower shell course forging 03 of the pressure vessel heat treated as shown in Table A-1. The Rotterdam Dockyard Company also supplied a weldment made from sections of forging 03 and adjoining intermediate shell course forging 04 using weld wire representative of that used in the original fabrication. The forgings were produced by Rheinstahl Huttenwecke. The heat treatment history and quantitative chemical analysis of the pressure vessel surveillance material are presented in Tables A-1 and A-2, respectively.

Table A-1. Heat Treatment History

| <u>Material</u> | <u>Temperature, F</u> | <u>Time, h</u> | <u>Coolant</u> |
|---|---------------------------|----------------|---------------------------|
| Lower shell forging 03, Heat No. 990400/292332 | 1616-1725 | 2.5 | Water-quenched |
| | 1202-1292 | 7.5 | Furnace-cooled to 842F |
| | 1130 ± 25 | 14.75 | Furnace-cooled |
| Weld metal | 1130 ± 25 | 10.75 | Furnace-cooled |

Table A-2. Quantitative Chemical Analysis, wt %

| <u>Element</u> | <u>Forging 03 heat No. 990400/292332¹ (Westinghouse^a)</u> | <u>Rotterdam dock analysis</u> | <u>W weld metal analysis</u> |
|----------------|---|--|----------------------------------|
| C | 0.20 | 0.19 | 0.06 |
| S | 0.011 | 0.014 | 0.012 |
| N ₂ | 0.015 | -- | 0.015 |
| Co | 0.020 | -- | 0.006 |
| Cu | 0.16 | 0.15 | 0.086 |
| Si | 0.26 | 0.22 | 0.35 |
| Mo | 0.61 | 0.63 | 0.49 |
| Ni | 0.79 | 0.80 | 0.11 |
| Mn | 0.68 | 0.68 | 1.29 |
| Cr | 0.30 | 0.30 | 0.025 |
| V | 0.037 | 0.02 | 0.001 |
| P | 0.019 | 0.010 | 0.020 |
| Sn | 0.017 | -- | 0.003 |
| Al | 0.021 | -- | 0.009 |

^aAll elements not listed are less than 0.010 wt %.

APPENDIX B
Preirradiation Tensile Data¹

Table B-1. Preirradiation Tensile Properties of Forging Material (Base Metal) and Weld Metal¹

| <u>Test temperature, F</u> | <u>Yield strength, ksi</u> | <u>Ultimate tensile strength, ksi</u> | <u>Percent total elongation</u> | <u>Percent reduction in area</u> |
|----------------------------|----------------------------|---------------------------------------|---------------------------------|----------------------------------|
| <u>Forging Material</u> | | | | |
| Room | 70.1 | 92.4 | 18.8 | 60.7 |
| Room | 71.3 | 92.7 | 18.8 | 57.0 |
| Average | 70.7 | 92.5 | 18.8 | 58.8 |
| 550 | 58.0 | 87.2 | 20.6 | 52.0 |
| 550 | 53.1 | 85.3 | 26.0 | 57.0 |
| Average | 55.6 | 86.2 | 23.3 | 54.5 |
| <u>Weld Metal</u> | | | | |
| Room | 63.2 | 78.3 | 18.9 | 71.0 |
| Room | 65.2 | 80.4 | 19.5 | 71.0 |
| Average | 64.2 | 79.4 | 19.2 | 71.0 |
| 550 | 60.2 | 76.9 | 20.0 | 63.0 |
| 550 | 61.7 | 80.5 | 18.0 | 57.0 |
| Average | 60.9 | 78.7 | 19.0 | 60.0 |

APPENDIX C
Preirradiation Charpy Impact Data¹

Table C-1. Preirradiation Charpy V-Notch Impact Data for
 North Anna Unit 1 Reactor Pressure Vessel
 Lower Shell Forging 03, Heat No. 990400/
 292332, Axial Orientation¹

| Test temp, F | Impact energy, ft-lb | Lateral expansion, mils | Shear fracture, % |
|--------------------|----------------------------|-------------------------------|-------------------------|
| -15 | 16 | 7 | 10 |
| -15 | 17 | 10 | 10 |
| -15 | 15 | 10 | 10 |
| 45 | 31.5 | 21 | 35 |
| 45 | 30 | 20 | 35 |
| 45 | 25 | 21 | 30 |
| 75 | 47.5 | 37 | 30 |
| 75 | 43.5 | 37 | 23 |
| 75 | 47.5 | 33 | 27 |
| 105 | 62.5 | 50 | 55 |
| 105 | 56.5 | 50 | 55 |
| 105 | 59 | 50 | 55 |
| 150 | 80.5 | 66 | 90 |
| 150 | 84.5 | 100 | 72 |
| 150 | 67.5 | 78 | 62 |
| 210 | 85 | 69 | 100 |
| 210 | 82.5 | 68 | 100 |
| 210 | 86.5 | 73 | 100 |

Table C-2. Preirradiation Charpy V-Notch Impact Data for
 North Anna Unit 1 Reactor Pressure Vessel
 Lower Shell Forging 03, Heat No. 990400/
 292332, Tangential Orientation¹

| Test temp, F | Impact energy, ft-lb | Lateral expansion, mils | Shear fracture, % |
|--------------------|----------------------------|-------------------------------|-------------------------|
| -15 | 30 | 21 | 9 |
| -15 | 9 | 5 | 0 |
| -15 | 19 | 16 | 3 |
| 40 | 66 | 48 | 40 |
| 40 | 84 | 60 | 45 |
| 40 | 78 | 59 | 56 |
| 74 | 96.5 | 67 | 38 |
| 74 | 101 | 74 | 64 |
| 74 | 73.5 | 59 | 38 |
| 125 | 116 | 74 | 77 |
| 125 | 115 | 78 | 92 |
| 125 | 99 | 67.5 | 79 |
| 170 | 143 | 80 | 100 |
| 170 | 147 | 83 | 100 |
| 170 | 144 | 81 | 100 |
| 210 | 126.5 | 88 | 100 |
| 210 | 123 | 84.5 | 100 |
| 210 | 127 | 80 | 100 |

Table C-3. Preirradiation Charpy V-Notch Impact Data for
 North Anna Unit 1 Reactor Pressure Vessel
 Core Region Weld Heat-Affected Zone Material

| Test temp, F | Impact energy, ft-lb | Lateral expansion, mils | Shear fracture, % |
|--------------------|----------------------------|-------------------------------|-------------------------|
| -125 | 21 | 13 | 9 |
| -125 | 4.5 | 2.5 | 5 |
| -125 | 13 | 6 | 5 |
| -80 | 25.5 | 13 | 3 |
| -80 | 76.5 | 47 | 29 |
| -80 | 53 | 21 | 18 |
| -25 | 22.5 | 13 | 18 |
| -25 | 47 | 26 | 23 |
| -25 | 31.5 | 15 | 13 |
| 40 | 104 | 65 | 81 |
| 40 | 62 | 43.5 | 45 |
| 40 | 78.5 | 46 | 42 |
| 100 | 156.5 | 78 | 100 |
| 100 | 127.5 | 81 | 79 |
| 100 | 125.5 | 73 | 90 |
| 170 | 152.5 | 72 | 100 |
| 170 | 166 | 82 | 100 |
| 170 | 109 | 74 | 100 |

Table C-4. Preirradiation Charpy V-Notch Impact Data for
North Anna Unit 1 Reactor Pressure Vessel
Core Region Weld Metal

| Test temp, F | Impact energy, ft-lb | Lateral expansion, mils | Shear fracture, % |
|--------------------|----------------------------|-------------------------------|-------------------------|
| -110 | 9 | 9 | 0 |
| -110 | 5 | 9 | 0 |
| -110 | 13 | 7 | 0 |
| 0 | 74.5 | 61 | 48 |
| 0 | 58 | 52 | 54 |
| 0 | 60 | 70 | 43 |
| 48 | 37.5 | 39.5 | 31 |
| 48 | 40 | 45 | 51 |
| 48 | 42 | 49.5 | 40 |
| 75 | 83 | 68 | 79 |
| 75 | 81 | 71.5 | 81 |
| 75 | 49.5 | 50 | 65 |
| 175 | 106 | 89 | 100 |
| 175 | 106 | 88 | 100 |
| 175 | 94 | 76 | 96 |
| 250 | 87 | 79 | 100 |
| 250 | 90.5 | 81 | 100 |
| 250 | 84.5 | 77 | 100 |

Figure C-1. Charpy Impact Data From Unirradiated Base Metal, Axial Orientation

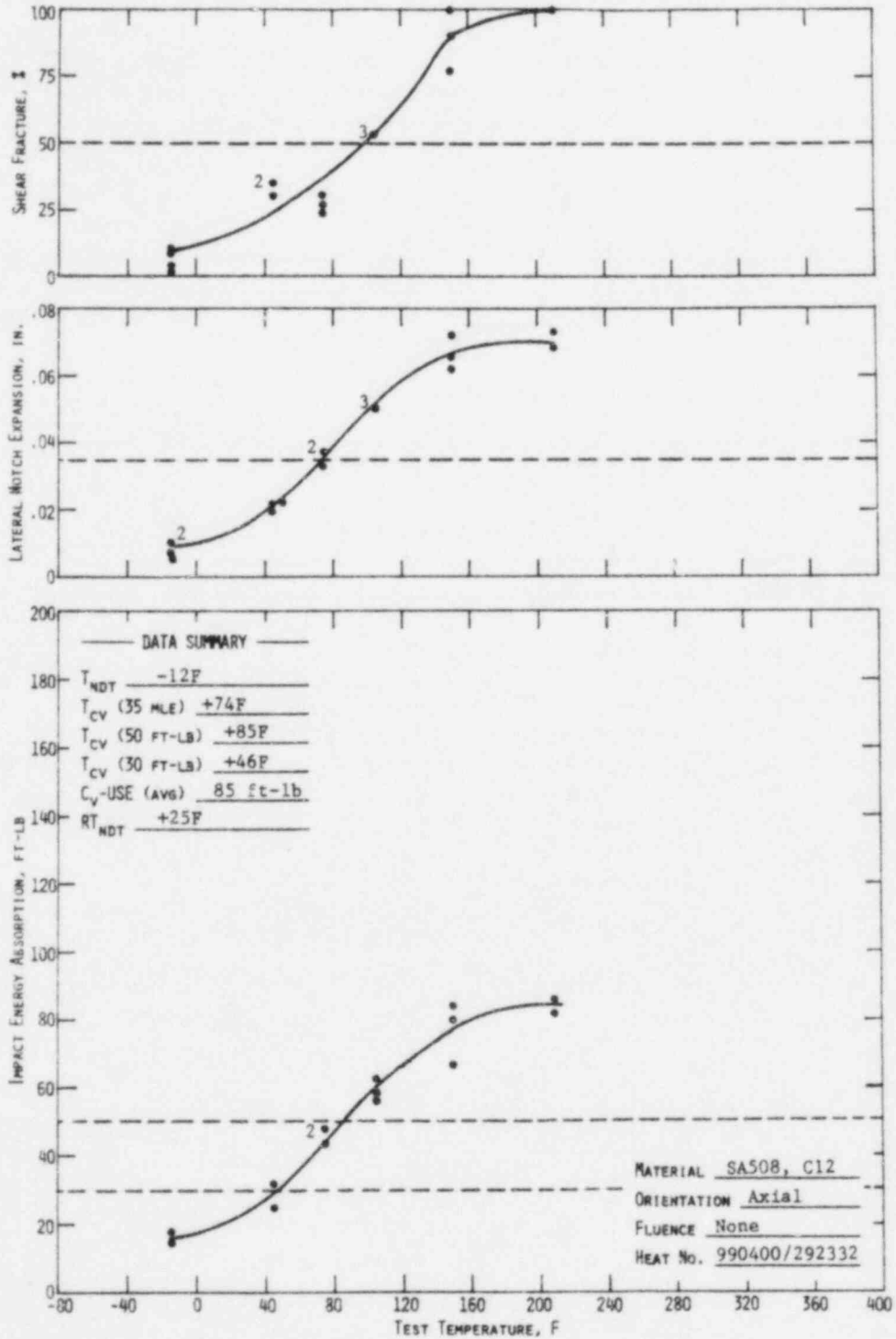


Figure C-2. Charpy Impact Data From Unirradiated Base Metal, Tangential Orientation

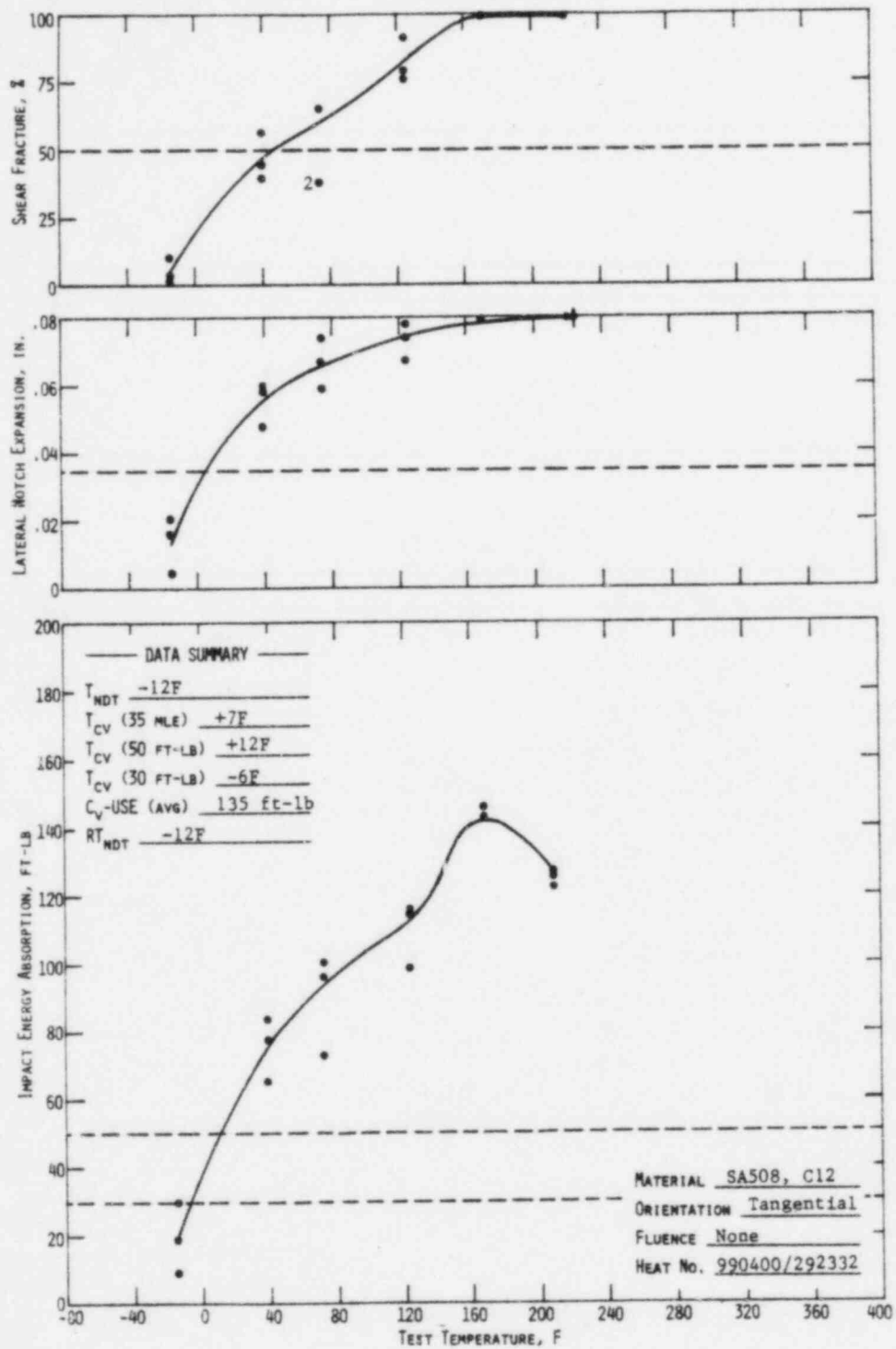


Figure C-3. Charpy Impact Data From Unirradiated Weld Metal

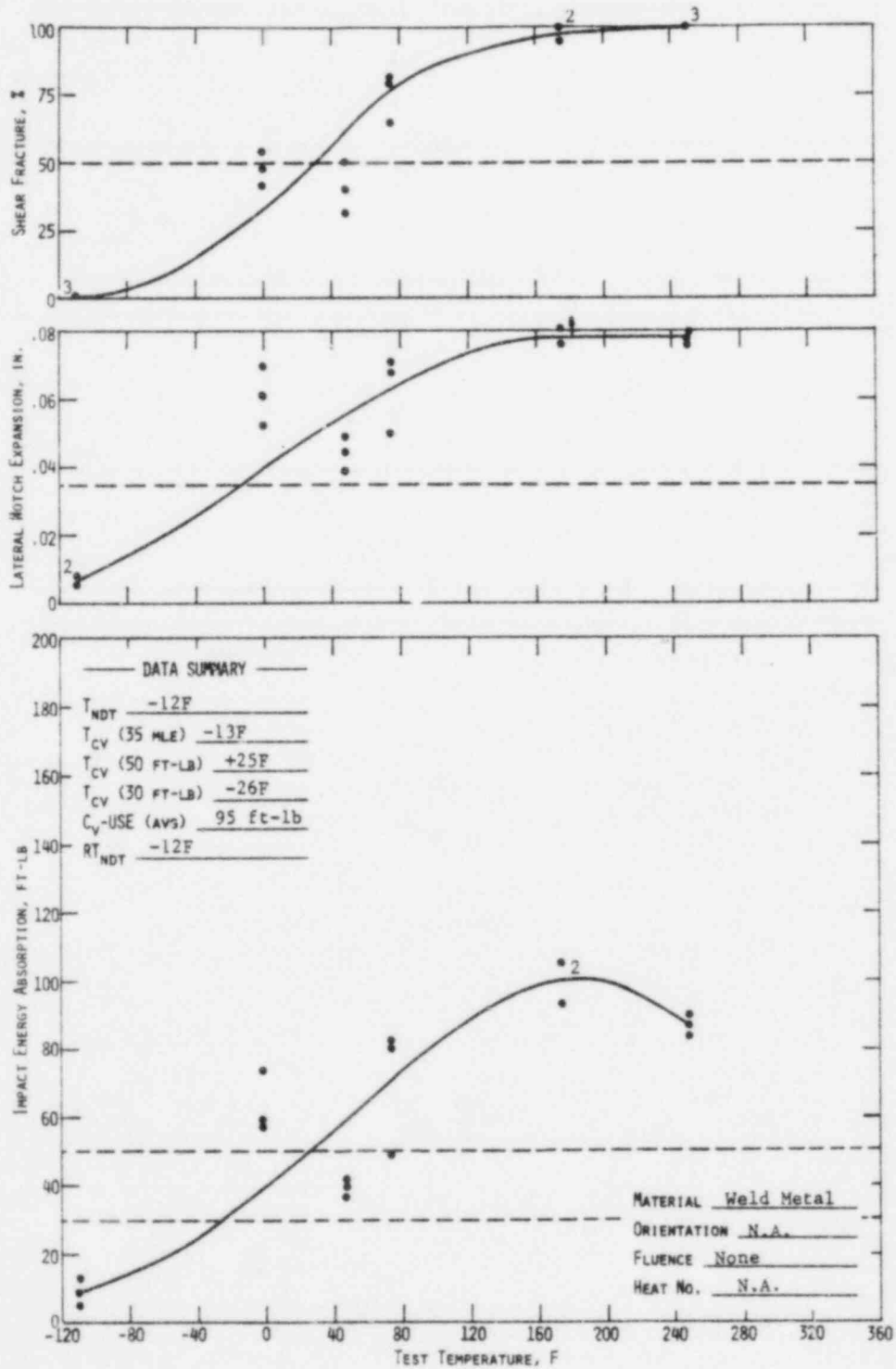
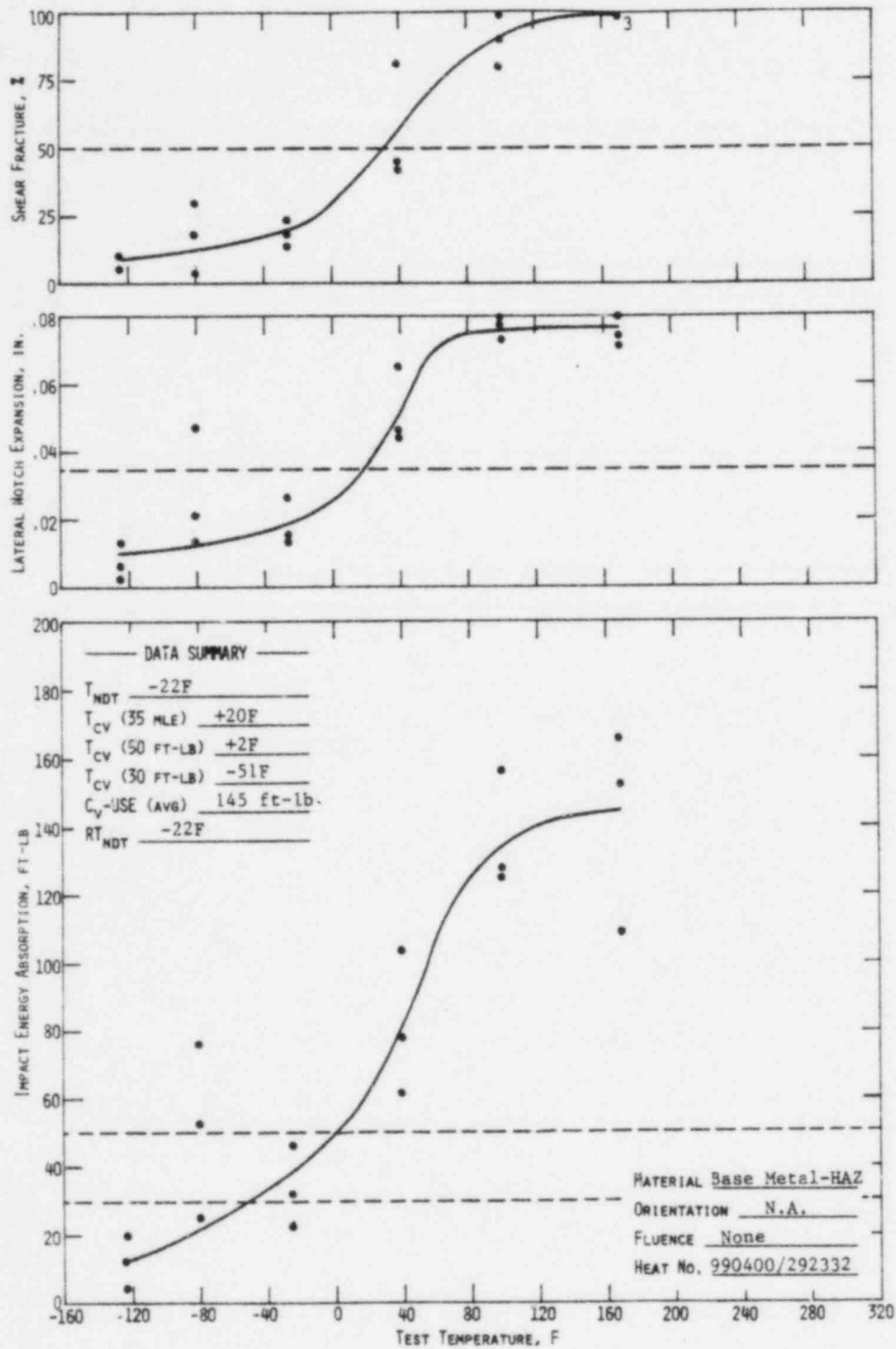


Figure C-4. Charpy Impact From Unirradiated Base Metal, Heat-Affected-Zone



APPENDIX D
Threshold Detector Information

Table D-1. North Anna Neutron Dosimeters - Capsule V Irradiation
 Ended September 25, 1979, 24:00

| Dosimeter Material | Location | Mass (grams) | Reaction | Nuclide | Nuclide Activity(μCi) | Activity/Gram of Material($\mu\text{Ci/g}$) ^(a) | Activity/Gram of Target($\mu\text{Ci/g}$) ^(b,c) | |
|-----------------------------------|------------------------|-------------------------------------|--|--|------------------------------------|--|--|------------------------|
| Iron | T-Fe | .0524 | $^{54}\text{Fe}(n,p)^{54}\text{Mn}$ | ^{54}Mn | 2.79 | 53.3 | 916 | |
| | | | $^{58}\text{Fe}(n,\gamma)^{59}\text{Fe}$ | ^{59}Fe | 6.03 | 115. | 34,800 | |
| | MT-Fe | .0544 | $^{54}\text{Fe}(n,p)^{54}\text{Mn}$ | ^{54}Mn | 2.76 | 50.8 | 873 | |
| | | | $^{58}\text{Fe}(n,\gamma)^{59}\text{Fe}$ | ^{59}Fe | 6.58 | 121. | 36,700 | |
| | Mid-Fe | .0442 | $^{54}\text{Fe}(n,p)^{54}\text{Mn}$ | ^{54}Mn | 2.35 | 53.1 | 912 | |
| | | | $^{58}\text{Fe}(n,\gamma)^{59}\text{Fe}$ | ^{59}Fe | 5.13 | 116. | 35,200 | |
| | MB-Fe | .0482 | $^{54}\text{Fe}(n,p)^{54}\text{Mn}$ | ^{54}Mn | 2.42 | 50.2 | 863 | |
| | | | $^{58}\text{Fe}(n,\gamma)^{59}\text{Fe}$ | ^{59}Fe | 5.40 | 112 | 33,900 | |
| | B-Fe | .0368 | $^{54}\text{Fe}(n,p)^{54}\text{Mn}$ | ^{54}Mn | 1.91 | 52.0 | 893 | |
| | | | $^{58}\text{Fe}(n,\gamma)^{59}\text{Fe}$ | ^{59}Fe | 4.34 | 118. | 35,800 | |
| | Cobalt-Aluminum (Bare) | T-Co | .0082 | $^{59}\text{Co}(n,\gamma)^{60}\text{Co}$ | ^{60}Co | 2.01 | 245. | 163,000 ^(d) |
| | | B-Co | .0070 | $^{59}\text{Co}(n,\gamma)^{60}\text{Co}$ | ^{60}Co | 1.81 | 258. | 172,000 |
| Cobalt-Aluminum (Cadmium Covered) | T-Co | .0064 | $^{59}\text{Co}(n,\gamma)^{60}\text{Co}$ | ^{60}Co | 0.0568 | 88.8 | 59,200 ^(d) | |
| | B-Co | .0063 | $^{59}\text{Co}(n,\gamma)^{60}\text{Co}$ | ^{60}Co | 0.556 | 88.3 | 58,900 | |
| Copper | MT-Cu | .0532 | $^{63}\text{Cu}(n,\alpha)^{60}\text{Co}$ | ^{60}Co | 0.0745 | 1.40 | 2.04 | |
| | Mid-Cu | .0512 | $^{63}\text{Cu}(n,\alpha)^{60}\text{Co}$ | ^{60}Co | 0.0758 | 1.48 | 2.16 | |
| | MB-Cu | .0582 | $^{63}\text{Cu}(n,\alpha)^{60}\text{Co}$ | ^{60}Co | 0.0815 | 1.40 | 2.04 | |
| Nickel | MT-Ni | .0486 | $^{58}\text{Ni}(n,p)^{58}\text{Co}$ | ^{58}Co | 51.0 | 1050. | 1550. | |
| | | | $^{60}\text{Ni}(n,p)^{60}\text{Co}$ | ^{60}Co | 0.100 | 2.05 | 7.84 | |
| | Mid-Ni | .0534 | $^{58}\text{Ni}(n,p)^{58}\text{Co}$ | ^{58}Co | 57.7 | 1080. | 1590. | |
| | | | $^{60}\text{Ni}(n,p)^{60}\text{Co}$ | ^{60}Co | 0.115 | 2.15 | 8.22 | |
| | MB-Ni | .0576 | $^{58}\text{Ni}(n,p)^{58}\text{Co}$ | ^{58}Co | 59.3 | 1030. | 1520 | |
| | | $^{60}\text{Ni}(n,p)^{60}\text{Co}$ | ^{60}Co | 0.119 | 2.06 | 7.87 | | |

D-2

Table D-1. (Cont'd)

| Dosimeter Material | Location | Mass (grams) | Reaction | Nuclide | Nuclide Activity(μCi) | Activity/Gram of Material($\mu\text{Ci/g}$) ^(a) | Activity/Gram of Target($\mu\text{Ci/g}$) ^(b,c) |
|------------------------|-----------------|--------------|----------------------------|-------------------|------------------------------------|--|--|
| U_3O_8 | Dosimeter Block | 0.0136 | $^{238}\text{U}(n,F)F.P.$ | ^{95}Zr | 0.974 | 71.6 | 84.4 ^(e) |
| | | | | ^{103}Ru | 1.24 | 91.2 | 108. |
| | | | | ^{106}Ru | 0.317 | 23.3 | 27.5 |
| | | | | ^{137}Cs | 0.0378 | 2.78 | 3.28 |
| | | | | ^{141}Ce | .837 | 54.6 | 64.5 |
| | | | | ^{144}Ce | 0.589 | 43.3 | 51.1 |
| | | | | ^{95}Zr | 4.02 | 536. | 608 ^(e) |
| NpO_2 | Dosimeter Block | 0.0075 | $^{237}\text{Np}(n,F)F.P.$ | ^{103}Ru | 4.10 | 547 | 621 |
| | | | | ^{106}Ru | 0.900 | 120 | 136 |
| | | | | ^{137}Cs | 0.141 | 18.8 | 21.3 |
| | | | | ^{141}Ce | 6.63 | 884. | 1000 |
| | | | | ^{144}Ce | 1.99 | 266. | 302. |
| | | | | ^{125}Sb | 0.0244 | 3.25 | 3.69 |

(a) The materials are defined to be iron, cobalt, copper, nickel, U_3O_8 and NpO_2 .

(b) The target nuclides are listed on the left side under the column headed REACTION.

(c) The following weight percents were used to calculate the activity per gram of target nuclide:

| | |
|------------------|-----------|
| ^{54}Fe | 5.82 wt% |
| ^{58}Fe | 0.33 wt% |
| ^{59}Co | 100. wt% |
| ^{63}Cu | 68.5 wt% |
| ^{58}Ni | 67.77 wt% |
| ^{60}Ni | 26.16 wt% |

(d) Data provided by Art Lowe indicate the cobalt-aluminum wire is 0.15% cobalt

(e) Westinghouse-supplied data lists the quantity of ^{238}U as 12 mg and the quantity of ^{237}Np as 17.1 mg. Only part of each was recovered from the capsules. Both are stated to be "99.9% pure". Using the formula weights for $^{238}\text{U}_3\text{O}_8$ and $^{237}\text{NpO}_2$ yields target weight fractions of 0.848 and 0.881.

Table D-2. Dosimeter Activation Cross Sections ^(a)

| G | Energy range, Mev | | ²³⁷ Np | ²³⁸ U | ⁵⁸ Ni | ⁵⁴ Fe | ⁶³ Cu |
|----|----------------------|--------|-------------------|------------------|------------------|------------------|------------------|
| 1 | 13.3 | -15.0 | 2.323 | 1.050 | 0.4830 | 0.4133 | 4.478 (-2) |
| 2 | 10.0 | -12.2 | 2.341 | 0.9851 | 0.5735 | 0.4728 | 5.361 (-2) |
| 3 | 8.18 | -10.0 | 2.309 | 0.9935 | 0.5981 | 0.4772 | 3.378 (-2) |
| 4 | 6.36 | -8.18 | 2.093 | 0.9110 | 0.5921 | 0.4714 | 1.246 (-2) |
| 5 | 4.96 | -6.36 | 1.541 | 0.5777 | 0.5223 | 0.4321 | 3.459 (-3) |
| 6 | 4.06 | -4.96 | 1.532 | 0.5454 | 0.4146 | 0.3275 | 6.348 (-4) |
| 7 | 3.01 | -4.06 | 1.614 | 0.5340 | 0.2701 | 0.2193 | 7.078 (-5) |
| 8 | 2.46 | -3.01 | 1.689 | 0.5272 | 0.1445 | 0.1080 | 3.702 (-6) |
| 9 | 2.35 | -2.46 | 1.695 | 0.5298 | 9.154 (-2) | 5.613 (-2) | 6.291 (-7) |
| 10 | 1.83 | -2.35 | 1.677 | 0.5313 | 4.856 (-2) | 2.940 (-2) | 1.451 (-7) |
| 11 | 1.11 | -1.83 | 1.596 | 0.2608 | 1.180 (-2) | 2.948 (-3) | 1.317 (-9) |
| 12 | 0.55 | -1.11 | 1.241 | 9.845 (-3) | 6.770 (-4) | 6.999 (-5) | 0 |
| 13 | 0.111 | -0.55 | 0.2341 | 2.432 (-4) | 1.174 (-6) | 1.578 (-8) | 0 |
| 14 | 0.0033 | -0.111 | 0.0069 | 3.616 (-5) | 1.023 (-7) | 1.389 (-9) | 0 |

(a) ENDF/BV values flux-weighted with a fission spectrum combined with a 1/E intermediate energy distribution.

APPENDIX E
LRC-TP-78

1. Introduction

- 1.1 This Technical Procedure outlines a method for the static tension testing of metallic solid round cross-sectional specimens at both room and elevated temperatures. The test shall provide data for the evaluation of yield and tensile strengths, approximate elastic modulus, and various ductility parameters. The room temperature portion of this procedure is in accordance with ASTM Method E8-78 unless otherwise specified. ASTM Method E21-70 was the guide for the elevated temperature portion and actual conformance will be indicated where applicable.
- 1.2 This procedure is designed to document the commitments made by the testing organization during the performance of the tension test. Specifically, these commitments are in regards to operator qualification, equipment calibrations, test and analysis procedures, and the test record.
- 1.3 Results obtained from specimens tested according to this procedure will be acceptable for B&W's Reactor Vessel Material Surveillance Program (RVSP). This procedure has been written primarily for the purpose of testing the two specimens currently in the surveillance program: A 0.357 inch diameter specimen and a 0.180 inch diameter specimen.
- 1.4 The scope of this procedure does not include detailed instrument settings and test parameters required by the person who performs the test. Mention will be made, however, whenever a referenced ASTM Method contains information of interest to said person.

Note: The latest edition of the applicable ASTM methods supersedes those listed in this procedure.

2. Operator Qualification

2.1 Individuals performing the static tension test shall be qualified by training and experience and shall have demonstrated competency to perform the tests in accordance with this procedure to the satisfaction of the LRC Project Leader.

3. Specimen

3.1 Specimen Geometry

The specimen shall be any round cross-sectional specimen. The gage length shall be four times the diameter of the specimen. The ends of the specimen outside the gage length shall be of a shape to fit the grips of the testing machine such that the loads are applied axially.

3.2 Specimen Preparation

In order to measure the deformation of the specimen, two fiducial marks shall be imprinted at the boundaries of the gage length. These marks may be stamped lightly with a punch, scribed lightly with dividers or a razor, or drawn with ink, as required by the LRC Project Leader. Care should be taken to place the marks with the same angular orientation with respect to one another.

4. Equipment

4.1 Testing Machine

The machine used for tension testing shall have sufficient capacity to load each specimen to failure.

4.2 Grips

The machine shall be equipped with suitable gripping devices to transmit the applied load to the test specimen. To minimize bending and ensure uniaxial loading within the gage length, the axis of the specimen shall coincide with the center line of the heads of the testing machine.

4.3 Axial Extension Instrument

An appropriate set of equipment for measuring axial extension shall be used to an elongation greater than that corresponding to the 0.2% off-set yield point. Afterwards, axial extension may be obtained from the stroke output of the testing machine.

4.4 Heating Element

The heating apparatus shall provide uniform heating along the gage length of the test specimen to within ± 5 F (± 3 C) of the nominal test temperature at the onset of the test. This paragraph conforms to ASTM Method E21-70, section 7.4.4.

4.5 Temperature Measurement Apparatus

The temperature measurement apparatus shall be of sufficient accuracy and sensitivity to monitor the test temperature within limits specified in 4.4. Temperature shall be measured with thermocouples in conjunction with potentiometers or voltmeters. This paragraph conforms to ASTM Method E21-70, sections 4.3.1 and 4.3.2.

4.6 Calibrations

4.6.1 Load

The load cell with its associated electronics shall be calibrated against standards traceable to the National Bureau of Standards (NBS) at least annually by a qualified service representative. The calibration of the electronics will be checked at the onset of each day of testing by checking the electrical output of the system when under the stimulus of a fixed calibration voltage (which simulates a load).

4.6.2 Stroke

The stroke (displacement) monitoring portion of the tension test machine shall be calibrated at least annually by a qualified service representative against standards traceable to the NBS.

4.6.3 Strain

The strain monitoring portion of the tension test apparatus is composed of four parts -- a 4-pole axial extensometer, a clip-on strain gaged extension transducer (with cable), a signal conditioning unit, and output recorder. The 4-pole extensometer will not require calibration. The transducer, signal conditioner, and output recorder shall be calibrated at least annually, although not necessarily concurrently, against standards traceable to the NBS. The calibration of the transducer, signal conditioner, and output recorder shall be checked as a unit at the onset of each day of testing. This shall be done by the comparison between the output recorder's response to the movement of an NBS traceable micrometer.

4.6.4 Temperature

The electronics portion of the temperature measurement system shall be calibrated at least annually against standards traceable to the NBS. The thermocouple alone need not receive calibration, however the thermocouple-electronics system shall be checked at least daily against an ASTM industrial grade (or better) thermometer at ambient temperature. The thermocouple wire shall be replaced at least monthly.

4.6.5 Diametral Measurement

The instrument used for diametral measurement shall be calibrated at least annually against standards traceable to the NBS.

5. Test and Specimen Parameters

5.1 Speed of Testing

Testing shall be performed in stroke (displacement) or strain control. Speeds [in distance/time or distance/(gage length x time)] shall be designated by the LRC Project Leader. Speeds may be increased after the 0.2% offset yield point is passed, also by designation of the LRC Project Leader.

5.2 Temperature

The nominal test temperature shall be designated by the LRC Project Leader. The testing shall not begin until thermal equilibrium is reached. The time of holding at temperature prior to the start of the test shall not be less than 20 minutes.

5.3 Specimen Measurement

The cross-sectional area, A_o , of the specimen shall be determined by the following equation:

$$A_o = \frac{\pi}{4} (OD_o)^2$$

where OD_o is the outside diameter at the gage section before testing. The value, OD_o , shall be either measured directly from the specimen or taken from an existing data sheet.

5.4 Test Record

The test record shall include a graph of load-strain (load-displacement) behavior. The load and strain (displacement) ranges shall be selected to provide adequate data resolution for the specified test conditions. Pertinent procedural parameters shall be listed by the operator on the Static Tension Test Record Report (see attachment).

6. Analysis Procedure

The results listed below shall be determined by the methods described in ASTM Method E8-69. For convenience, summaries of these methods are described below.

6.1 Uniform Strain

Strain shall be reported as the increase in the gage length expressed as a percentage of the initial gage length, as follows:

$$\epsilon_U = \left(\frac{\Delta l}{l_0} \right) \times 100\%$$

where:

| | | |
|--------------|-------------------------------|-----------------|
| ϵ_U | = Uniform strain, % | (dimensionless) |
| Δl | = Increase in the gage length | (in.) |
| l_0 | = Initial gage length | (in.) |

The increase in the gage length is found from the load-elongation chart. Uniform strain includes all elongation which occurs until the maximum load is reached. Should the extensometer be removed before the maximum load is reached, the gage length (after removal) shall be the original length of the reduced diameter section.

Both plastic uniform strain and elastic strain data are available from the load-strain chart. Uniform strain may be reported either as a summation of the two, or plastic uniform strain alone, to the preference of the LRC project leader. In either case, the type of strain reported shall be recorded on the Static Tension Test Record Report (see attachment).

6.2 Total Elongation

The total elongation includes the entire specimen deformation within the specimen after its failure. The equation to be used for the determination of total elongation is the same as that given in Section 6.1 (Uniform Strain), but with ϵ_T (total strain) substituted for ϵ_U . The increase in the gage length (Δl) shall be found by placing the broken ends of the specimen together and measuring the distance between fiducial marks. From this measurement is subtracted the original distance between the marks giving Δl .

6.3 Yield Strength

The yield strength shall be determined by the 0.2% offset method, as follows:

$$\sigma_{YS} = P_{0.2\%}/A_o$$

where:

$$\begin{aligned}\sigma_{YS} &= 0.2\% \text{ offset yield stress or strength} && (\text{psi}) \\ P_{0.2\%} &= \text{load at 0.2\% offset strain} && (\text{lbs}) \\ A_o &= \text{original cross sectional area} && (\text{in.}^2)\end{aligned}$$

The load at 0.2% offset strain ($P_{0.2\%}$) is found as follows. A straight line is drawn through the elastic portion of the curve on the load-strain chart. (The slope of this line approximates the material's elastic modulus.)

The increase in the gage length corresponding to 0.2% strain is calculated as follows:

$$\Delta l_{0.2\%} = (0.002) l_o$$

where:

$$\Delta l_{0.2\%} = \text{increase in the gage length at 0.2\% strain (in.)}$$

An offset of this amount relative to the elastic line is then plotted along the abscissa. A second line, parallel to the first but passing through the 0.2% offset strain point, is drawn on the chart. At the point where this line intersects the load-strain curve, the load ($P_{0.2\%}$) can be determined.

6.4 Tensile Strength

The tensile strength shall be calculated as follows:

$$\sigma_{TS} = P_{MAX}/A_o$$

where:

$$\begin{aligned}\sigma_{TS} &= \text{tensile strength} && (\text{psi}) \\ P_{MAX} &= \text{maximum load sustained by specimen} && (\text{lbs}) \\ A_o &= \text{original cross-sectional area} && (\text{in.}^2)\end{aligned}$$

6.5 Reduction of Area

The reduction of area is the difference between the final cross-sectional area at the fracture and the original cross-sectional area expressed as a percentage of the original cross-sectional area. The final cross-sectional area is calculated from the final diameter, thus

$$A_f = \frac{\pi (OD_f)^2}{4}$$

where:

OD_f = the final diameter (in.)

The final diameter shall be taken by placing the broken specimen edges together and measuring the specimen at its smallest section. The reported OD_f shall be the average of not less than three measurements taken at different angular orientations. The reduction of area (RA) shall then be calculated as

$$RA = \left(\frac{A_f - A_o}{A_o} \right) \times 100\%$$

6.6 Report

- 6.6.1 The test report shall include a graph of load-strain (load-displacement) behavior. Test results shall be included on the Static Tension Test Record Report (see attachment).
- 6.6.2 Photographs, diagrams, or other exhibits requested by the LRC Project Leader shall be attached to the report and noted on the report.
- 6.6.3 Notes shall be made in a record book with regards to maintenance, adjustments and calibrations.

APPENDIX F
LRC-TP-80

1. Introduction

- 1.1 This Technical Procedure outlines a method for notched bar impact testing of metallic specimens using the Charpy apparatus for the evaluation of impact energy, percent shear fracture, and lateral expansion. ASTM Methods A370-77, E23-72, and 10 CFR 50 Appendix G are the governing documents. Deviations from and conformance to particular specifications are noted in the procedure.
- 1.2 This procedure is designed to document the commitments made by the testing organization during the performance of the Charpy test. Specifically, these commitments are in regards to operator qualification, equipment calibrations, test and analysis procedures, and the test record.
- 1.3 Results obtained from Charpy specimens tested according to this procedure shall be acceptable for B&W's Reactor Vessel Surveillance Program (RVSP).
- 1.4 The scope of this procedure does not include detailed instrument settings and test parameters required by the person who performs the test. Mention will be made, however, whenever a referenced ASTM Method contains information of interest to said person.

Note: The latest edition of the applicable ASTM methods supersedes those listed in this procedure.

2. Operator Qualification

2.1 Individuals performing the Charpy impact test shall be qualified by training and experience and shall have demonstrated competency to perform the tests in accord with this procedure to the satisfaction of the LRC Project Leader. This paragraph is in compliance with 10 CFR 50, Appendix G.

3. Specimen

3.1 Specimen Geometry

The specimen shall be a Charpy impact test specimen, Type A, that conforms to ASTM E23-72, Section 7 and ASTM A370-77, Section 20.2.1.

3.2 Number of Tests

ASTM Method A370-77, Section 20.1.2 states that a test shall be composed of three specimens taken from a single test coupon or location. Due to the scarcity of specimens, one specimen shall compose a test. Consistent with this, this procedure is also in violation of Section 22.1, which requires an arithmetic average of three specimens as the result of a test.

4. Equipment

4.1 Testing Machine

The Charpy impact test machine shall be a pendulum type of rigid construction and of capacity at least 125% of that required to break each specimen. The machine shall be rigidly mounted to either a concrete floor not less than 6 inches thick or a base of a weight at least 40 times that of the pendulum. The machine shall conform to specifications described in ASTM E23-72 Sections 4.1, 4.2.2, 4.2.3 and 4.2.4.

4.2 Self-Centering Tongs

A set of tongs as shown in Figure 12 of ASTM E23-72 shall be used to center the specimens within the testing machine's anvils. This conforms to ASTM Methods E23-72, Sections 4.2.1 and 8.3.

4.3 Instrumented System

The impact machine shall be equipped with a "Dynatup" strain-gaged instrumented tup, signal conditioning unit, and data storage unit suitable for recording both load and energy vs. time behavior.

4.4 Temperature Conditioning

The temperature conditioning aspects of the impact test shall be done in conformance with ASTM Methods E23-72 section 8.2 and Methods A370-77 section 21.3.

The temperature chamber shall be of liquid immersion type. The device used to measure the temperature of the bath shall be placed near the center of a group of the specimens. The fluid shall be agitated continuously. The temperature chambers shall have a grid raised at least 1" from the bottom upon which the specimens shall rest. The fluid shall be of sufficient depth so that the specimens when immersed shall be covered by at least 1".

4.4.1 Low Temperature Testing

For testing at temperatures between -196C and room temperature, the chamber must be capable of providing the nominal test temperature to within +0 and -1.5C (+0 and -3F).

4.4.2 High Temperature Testing

For testing at temperatures between room temperature and 260C, the chamber must be capable of providing the nominal test temperature to within +1.5C and -0 (+3F and 0).

4.5 Temperature Measurement

The temperature of the immersion baths shall be measured with industrial grade ASTM mercury-in-glass thermometers.

4.6 Lateral Expansion Measurement

Lateral expansion of the specimen after impact shall be measured with a dial indicator rigidly mounted to a fixture. The fixture shall provide reference supports for locating the broken specimen halves properly with respect to the dial indicator. The dial indicator shall be equipped with a flat anvil to provide proper contact with the specimen. This device shall conform to ASTM Method A370-77 Section 23.2.3.1.

4.7 Percent Shear Fracture Determination

Should the percent shear fracture be determined according to ASTM Method A370-77 Section 23.2.2.1, Method 1, the width and height of the fracture surface shall be measured with a dial caliper.

5. Inspections and Calibrations

5.1 Impact Machine

5.1.1 Initial Inspection

The impact machine shall conform to ASTM Methods E23-72, Sections 4 and 5 at the time of installation. These specifications and tolerances need not be inspected periodically unless the machine is disassembled, fails to indicate the proper energies when checked against standardized Watertown specimens, or is suspected of a deviation for any other reason.

5.1.2 Annual Calibration Check

The accuracy of the impact machine shall be checked against standardized specimens from the Army Materials and Mechanics Research Center (Watertown) at least annually. Should the machine be moved, repaired, adjusted, or should there exist any reason to doubt the accuracy of the results, then it shall be checked against Watertown specimens immediately, without regard to the time interval. This paragraph conforms to ASTM Method E23-72, Sections 6 and 11.

5.1.3 Daily Check

At least once daily, the machine shall be checked by a free swing of the pendulum. With the indicator at the initial position, a free swing of the pendulum shall indicate zero energy. This paragraph conforms to ASTM Methods E23-72 Section 8.1.

A second daily check may be mandated by the R&D Project Leader. An aluminum calibration specimen may be tested at room temperature in a manner otherwise identical to that used for subsequent tests.

5.2 Instrumented System

The data storage unit(s) of the instrumented impact system shall be calibrated at least annually against standards traceable to the National Bureau of Standards (NBS). The system as a whole will be checked by the comparison of the energy value as recorded by the instrumented system with that as indicated on the impact machine. This shall be done on a random basis, at least once daily.

5.3 Temperature Measurement

The thermometer used for temperature measurement shall be calibrated against standards traceable to the NBS within 3 months prior to the test.

5.4 Lateral Expansion Measurement

The dial indicator used for the measurement of lateral expansion shall be calibrated at least annually against standards traceable to the NBS.

5.5 Percent Shear Fracture Determination

Should a dial caliper be used in the determination of percent shear fracture, it shall be calibrated at least annually against standards traceable to the NBS.

6. Test Procedure

6.1 Temperature

The nominal test temperature for each test shall be designated by the LRC project leader. Specimens shall remain immersed in the liquid medium for not less than 5 minutes at low temperatures (less than room temperature) and not less than 10 minutes at high temperatures (greater than room temperature). This paragraph is in conformance with ASTM Method E23-72, Section 8.2 and Method A370-77, Section 21.3.

6.2 Placement of Specimens

Self-centering tongs shall be used in order to assure alignment of the specimen within the machine anvils. The specimen-gripping portion of the tongs shall be cooled or heated with the specimens, except when transferring the specimen into the test machine. This paragraph is in conformance with ASTM Method E23-72, Sections 8.2 and 8.3 and Method A370-77, Section 21.3.5.

6.3 Preparation of the Machine

The pendulum shall be placed in its latched position. The energy indicator shall be set at its maximum energy position. The "Dynatup" instrumented system and the computer data acquisition system shall be prepared to receive data.

6.4 Operation of the Test

The specimen shall be removed from the immersion bath with the tongs and centered between the machine's anvils. The pendulum shall then be released from its latched position. This entire operation shall be completed within 5 seconds. The preceding operational sequence conforms to ASTM Method E23-72, Section 8.4.1. Should the specimen fail to break, or jam in the machine, the procedure as outlined in ASTM Method E23-72, Sections 8.4.3 or 8.4.4 shall be followed. To prevent recording an erroneous value caused by jarring the indicator when locking the pendulum in its upright position, the energy value shall be read from the indicator prior to locking the pendulum for the next test. The preceding sentence is in conformance with ASTM Method E23-72, Section 8.4.5.

7. Analysis Procedure

7.1 Impact Energy

The Charpy Impact Energy shall be read to the nearest interger as indicated on the Charpy machine's energy indicator. The maximum energy signal on the oscilloscope (E_{amax}) shall be read to the nearest determinable value.

7.2 Determination of Lateral Expansion

Lateral expansion shall be measured according to ASTM Method A370-77, Section 23.2.3.1. The following is a synopsis of that section:

The broken specimen halves shall be retrieved and cleared of any burrs which may exist on the surface, other than the protrusions to be measured. The specimen halves shall be measured by individually placing them against the reference supports, with the protrusion against the gage anvil. Two measurements shall be made on each specimen half: one measurement on each side. The larger of the two measurements corresponding to a given specimen side is the expansion of that side of the specimen. Total lateral expansion is the sum of the larger measurements for the two sides.

7.3 Determination of Percent Shear Fracture

The determination of percent shear fracture shall be done in accordance with either Method (1) or (2) of ASTM Methods A370-77 Section 23.2.2.1. Method (1) involves the use of dial caliper in the measurement of either specimen half's fracture surface as shown in Figure 14 of Method A370-77. The measurements shall be used in conjunction with Table 4 of Method A370-77 to find the percent shear fracture. Method (2) involves the comparison of the appearance of the fracture surface with the comparator chart, Figure 14 of Method A370-77. The choice of Method (1) or (2) shall be made by the LRC project leader on an individual specimen basis.

7.4 Test Report

The test report shall be as shown in Figure 7.1 "Charpy Impact Test Record". This report shall include those results called for in ASTM Methods A370-77 Section 23.3 and ASTM Methods E23-72 Sections 10.1.4, 10.1.5, 10.1.6, and 10.1.7. The remaining information requested in ASTM Methods E23-72, Section 10 has been omitted from the test report as it is either superfluous or available elsewhere in the procedure.